

# Composite model-based estimate of the ocean carbon sink from 1959 to 2022

Jens Terhaar<sup>1,2</sup>

<sup>1</sup>Climate and Environmental Physics, Physics Institute, University of Bern, Bern, Switzerland

<sup>2</sup>Oeschger Centre for Climate Change Research, University of Bern, Bern, Switzerland

*Correspondence to:* Jens Terhaar (jens.terhaar@unibe.ch)

**Abstract.** The ocean takes up around one quarter of anthropogenically emitted carbon and is projected to remain the main carbon sink once global temperatures stabilize. Despite the importance of this natural carbon sink, estimates of its strength over the last decades remain uncertain, mainly due to too few and unevenly sampled observations and shortcomings in ocean models and their setups. Here, I present a composite model-based estimate of the annually averaged ocean carbon sink from 1959 to 2022 by combining the higher-frequency variability of the annually averaged estimates of the carbon sink from ocean models in hindcast mode and the long-term trends from fully coupled Earth System Models. Ocean models in hindcast mode reproduce the observed climate variability, but their spin-up strategy likely leads to too weak long-term trends, whereas fully coupled Earth System Models simulate their own internal climate variability but better represent long-term trends. By combining these two modelling approaches, I keep the strength of each approach and remove the respective weaknesses. This composite model-based estimate of the ocean carbon sink from 1959 to 2022 is  $125 \pm 8$  Pg C and is similar in magnitude but 70% less uncertain than the best estimate of the Global Carbon Budget.

## 1 Introduction

The ocean is a major natural sink of anthropogenic carbon (Broecker et al., 1979; Sarmiento et al., 1992; Maier-Reimer and Hasselmann, 1987) and took up around one quarter of carbon emissions from fossil fuels and land use change over the last decades (Friedlingstein et al., 2023; Terhaar et al., 2022; Müller et al., 2023; DeVries et al., 2023). Moreover, the ocean will continue taking up carbon over the 21<sup>st</sup> century (Terhaar et al., 2022) and beyond when temperatures are eventually stabilizing (Silvy et al., 2024). Despite the importance of the ocean carbon sink for the global carbon cycle and hence the global climate, large uncertainties exist with respect to the magnitude, variability, and trends of the ocean carbon sink (DeVries et al., 2023; Terhaar et al., 2024; Friedlingstein et al., 2023).

Observation-based annually-resolved estimates of the ocean carbon sink are built on direct observations of the partial pressure of CO<sub>2</sub> ( $p\text{CO}_2$ ) at the ocean surface (Fay et al., 2021). While being built on observations is a strength of these observation-based  $p\text{CO}_2$  products, it is also their weakness. As observations are scarce in space and time, they must be extrapolated by

methods relying among others on artificial intelligence and machine learning, for example neural networks (Landschützer et al., 2015). However, even these cutting-edge extrapolation methods introduce biases in the strength of the decadal variability (Gloege et al., 2021) and trends (Hauck et al., 2023a; Terhaar, 2024). The data scarcity and uneven spacing in the past is impossible to overcome and the question was raised if the different methods of extrapolating these observations have “hit the wall” (Gregor et al., 2019).

An alternative to observation-based  $p\text{CO}_2$  products are global ocean biogeochemical models (GOBMs) that are forced with historical atmospheric reanalysis data, atmospheric  $\text{CO}_2$ , and radiative forcing from other radiative agents. As GOBMs are forced with these historical data, they represent the observed internal climate variability at the ocean surface and hence the high-frequency variability of the annually averaged ocean carbon sink, i.e., inter-annual to sub-decadal variability. However, differences in the simulated carbon sink by GOBMs are caused by differences in the simulated circulation and carbonate chemistry in these models (Terhaar et al., 2024), as well as different ways of setting up these GOBMs, e.g., the lengths of the spin-up or different atmospheric  $\text{CO}_2$  during the pre-industrial spin-up (Terhaar et al., 2024). Moreover, using atmospheric forcing from sometime between 1959 and present, the period when atmospheric reanalysis data is provided, for the pre-industrial spin-up leads to a too warm pre-industrial ocean and hence too weak transient warming in GOBMs (Huguenin et al., 2022) and too weak deoxygenation (Takano et al., 2023). This too warm pre-industrial ocean and too weak ocean warming may also influence the ocean carbon sink and its trends through biases in the base state and transient changes in the stratification, solubility, or carbonate chemistry of the ocean. However, the sign and magnitude of that effect remains still unclear.

Another option to estimate the annually resolved ocean carbon sink are fully coupled Earth System Models (ESMs) that are also forced with historical atmospheric  $\text{CO}_2$  and radiative forcing from other radiative agents but dynamically simulate their atmosphere. Being dynamically coupled, ESMs do not simulate the phase of the observed internal climate variability and hence not the high-frequency variability of the annually averaged ocean carbon sink. However, ESMs from the most recent phase 6 of the coupled model intercomparison project (CMIP6) are all set up in a common way, having the same atmospheric  $\text{CO}_2$  during the pre-industrial spin-up and long enough spin-ups that allow the simulated ocean to reach its own equilibrium (Séférian et al., 2016). Furthermore, their pre-industrial atmospheric and ocean temperatures in ESMs are colder than their respective historical temperatures so that the simulated transient ocean warming aligns with observed ocean warming (Takano et al., 2023). Finally, the simulated global ocean carbon sink could be adjusted for their biases in the simulated ocean circulation and carbonate chemistry with observations (Terhaar et al., 2021c, 2022). Thus, ESMs from CMIP6 can be considered to robustly simulate the long-term trends of the ocean carbon sink and the externally-forced decadal variability, which is mostly driven by changes in the atmospheric  $\text{CO}_2$  growth rate (Terhaar, 2024; McKinley et al., 2020).

As both model estimates will not overcome their respective weaknesses in the near future, I here propose a new composite  
65 model-based estimate of the ocean carbon sink combining the inter-annual and sub-decadal variability of the ocean carbon  
sink from GOBMs and the externally forced decadal variability and long-term evolution of the ocean carbon sink from ESMs.  
The combined model-based estimate uses the strength and removes the weaknesses of the respective model estimates.

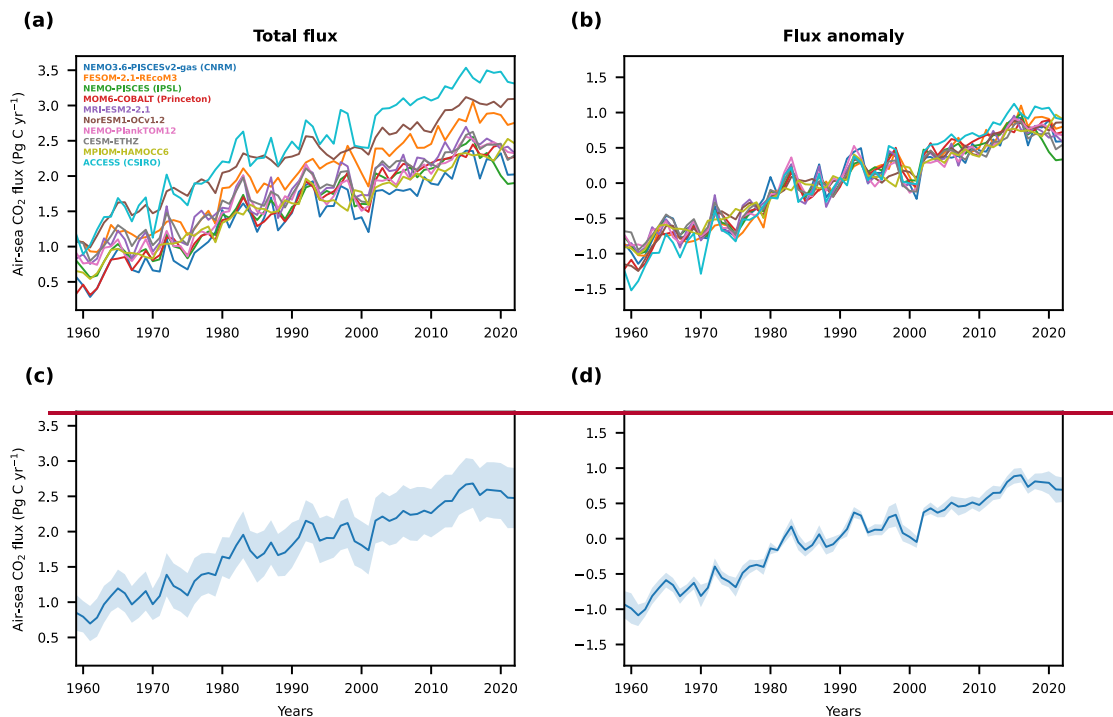
## 2 Results

### 2.1 A new composite model-based estimate

70 The 10 GOBMs from the Global Carbon Budget 2023 simulate a global ocean carbon sink from 1959 to 2022 of various  
strengths (Friedlingstein et al., 2023) (Fig. 1a, c) but the flux anomaly with respect to the mean simulated carbon sink over the  
entire period is almost indistinguishable across these GOBMs (Fig. 1b, d). Small common differences in the anomalies exist  
in 1985 and 1998 for the GOBMs NorESM1-OCv1.2 (Schwinger et al., 2016) and MPIOM-HAMOCC6 (Lacroix et al., 2021b)  
75 (Fig. 1b), likely because both use the NCEP reanalysis data (Kanamitsu et al., 2002) to force the simulations and not the  
JRA55-do (Tsujino et al., 2018) that is used by 7 GOBMs or ERA5 reanalysis datasets (Hersbach et al., 2020) that is used by  
one GOBM. Furthermore, the ACCESS (CSIRO) model (Law et al., 2017) simulates slightly weaker anomalies at the  
beginning of the simulation and stronger anomalies at the end of the simulations resulting in a larger trend of the anomalies  
over the entire period (Fig. 1b), although the models set-up is not different to the others (Friedlingstein et al., 2023). While the  
differences in the anomalies might be too small due to the small diversity in atmospheric forcing datasets, even the difference  
80 in the anomalies between GOBMs that use different forcing data is much smaller than the difference of the absolute fluxes  
simulated by GOBMs (Fig. 1a), which was removed by calculating the anomalies. Thus, the overall strong agreement in  
simulated anomalies of the global ocean carbon sink across these 10 GOBMs as expressed by the small multi-model standard  
deviation and between GOBMs that use different atmospheric forcing data gives high confidence in the multi-model mean  
estimate of the high-frequency variability of the simulated global ocean carbon sink by GOBMs (Fig. 1d).

85 As there are small inter-model differences in the simulated high-frequency variability of the global ocean carbon sink by the  
GOBMs and as it has been shown that ESMs largely agree in the magnitude and long-term trends of the global ocean carbon  
sink after adjusting for biases in ocean circulation and carbonate chemistry (Terhaar et al., 2022) and that the multi-model  
mean of ESMs can represent the externally forced decadal trends (Li and Ilyina, 2018; Terhaar, 2024), I here combine both  
90 model estimates to create a new composite model-based estimate of the global ocean carbon sink (Fig. 2c, Table A1). The  
high-frequency variability was here extracted by removing a spline fit (Enting, 1987) from the simulated carbon sink estimate  
from each GOBM separately (Friedlingstein et al., 2023) (Fig. 2b). The low-frequency variability and long-term trends were  
calculated by fitting a spline fit (Enting, 1987) to the bias-adjusted simulated carbon sink from each ESM separately (Terhaar  
et al., 2022) (Fig. 2a). The ESMs were forced with historical forcing until 2014 and with forcing from the Shared

95 Socioeconomic Pathways 1-2.6 (SSP1-2.6) (Riahi et al., 2017) after 2014 as the atmospheric CO<sub>2</sub> under that SSP (Meinshausen et al., 2020) is closest but still slightly above the observed atmospheric CO<sub>2</sub> (Lan et al., 2024). For the estimates of the long-term trend and short-term variabilities, it would have been possible to only use the members of the GOBM and ESM ensembles that have an ocean model component that is part of both ensembles to ensure consistency. However, I used all available GOBMs and ESMs as there is no indication that the short-term variability and long-term trend are linked and as the largest number of GOBMs and ESMs in each ensemble allows to best estimate both the short-term variability and long-term trend.  
 100 The uncertainty of the composite estimate is the combination of the multi-model standard deviation of the high-frequency variability from GOBMs and that of the long-term trends from ESMs, as well as the uncertainty from the spline fit (see Appendix for more details).



105

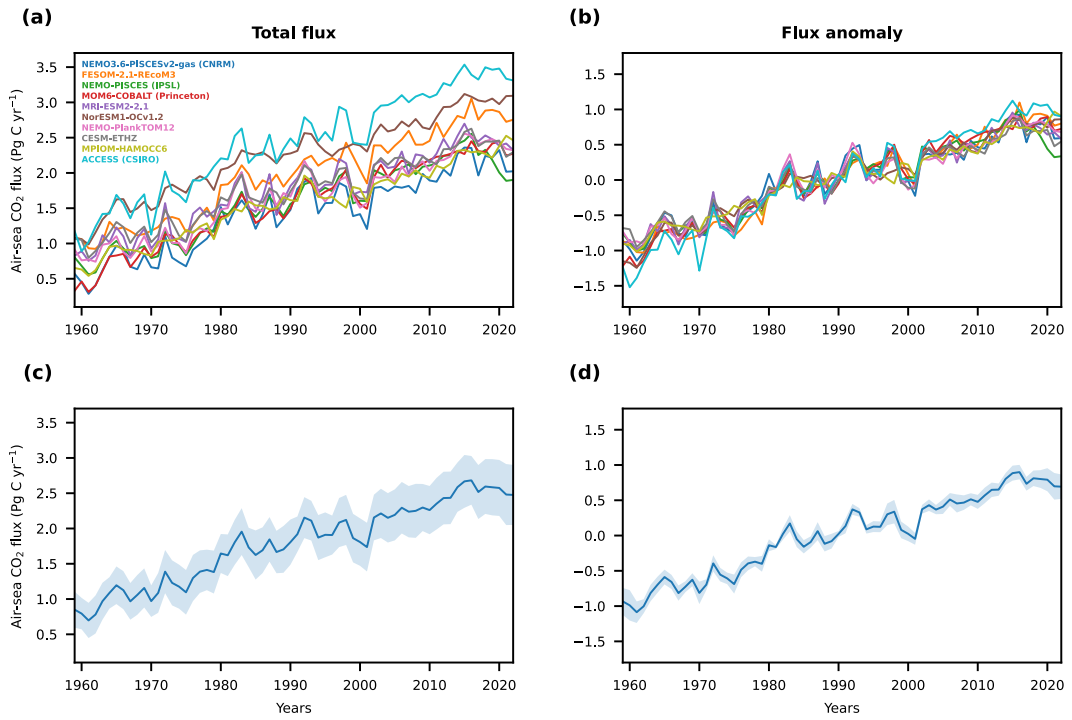
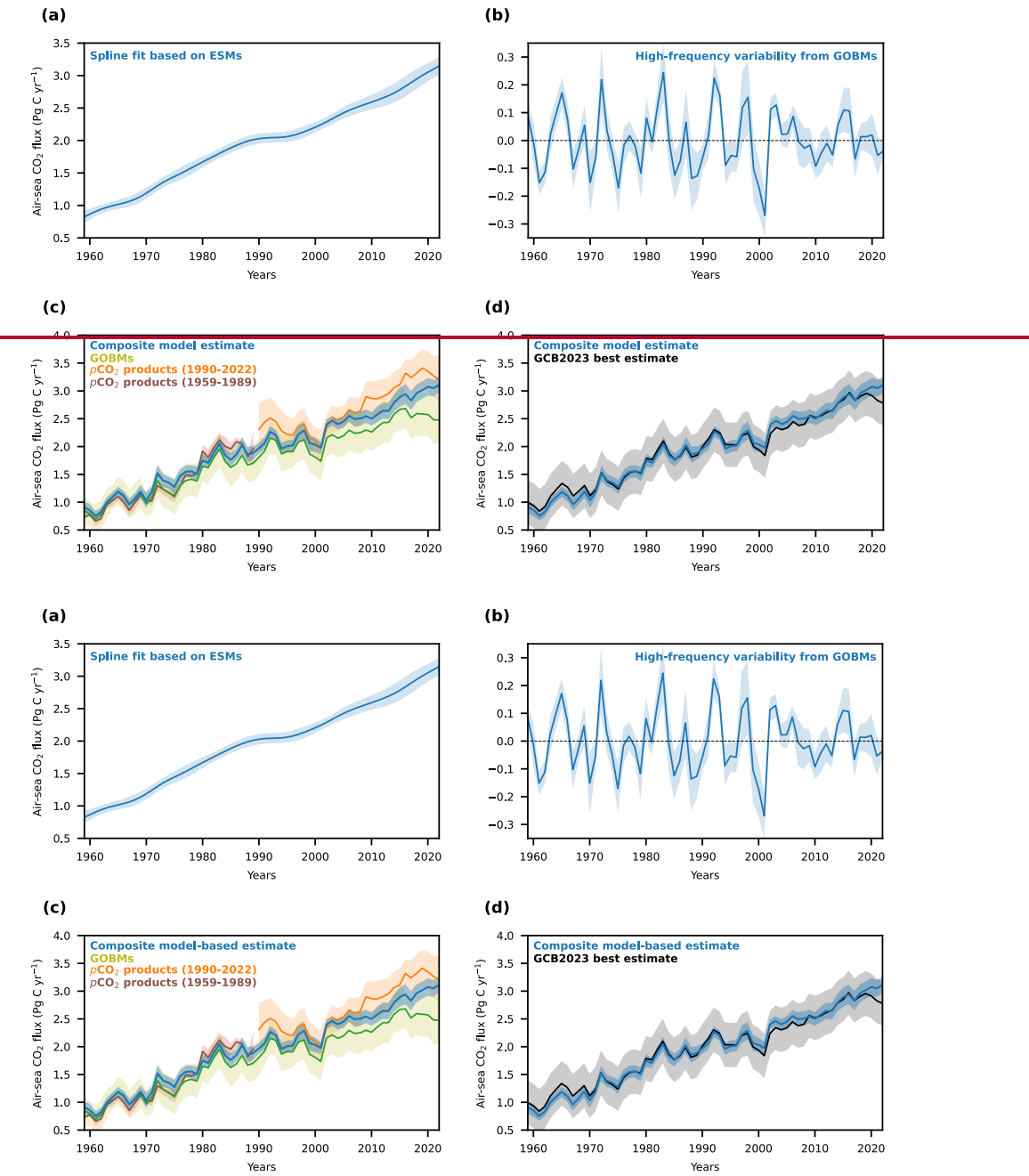


**Figure 1: Global ocean carbon sink and its anomaly as simulated by global ocean biogeochemical models.** The global ocean carbon sink as defined by the Global Carbon Budget 2023 (Friedlingstein et al., 2023) and (a) simulated by 10 global ocean biogeochemical models as well as (c) the multi-model mean and standard deviation. In addition, (b) the anomaly of the ocean carbon sink for the 10 global ocean biogeochemical models with respect to the mean flux from 1959 to 2022 in the respective GOBM, as well as (d) the multi-model mean and standard deviation of that anomaly are shown.

110

115

The ocean carbon sink estimated by this composite model-based estimate from 1959 to 2022 is  $125 \pm 8$  Pg C (Fig. 1c, Table A1). It increases from  $1.00 \pm 0.10$  Pg C yr<sup>-1</sup> in the 1960s to  $2.78 \pm 0.16$  Pg C yr<sup>-1</sup> in the 2010s. The increase of the ocean carbon sink slows down in the 1990s (decadal trend of  $0.10$  Pg C yr<sup>-1</sup> dec<sup>-1</sup>) and accelerates afterwards (decadal trends of  $0.55$  and  $0.56$  Pg C yr<sup>-1</sup> dec<sup>-1</sup> in the 2000s and 2010s) as expected from the trends in atmospheric CO<sub>2</sub> and the eruption of Mount Pinatubo in the early 1990s (McKinley et al., 2020; Fay et al., 2023; Terhaar, 2024).



125 **Figure 2: Composite model-based estimate of the ocean carbon sink and its two components.** (a) A spline fit to the ocean carbon sink as simulated by ESMs from Earth System Models and adjusted for biases in the ocean circulation and carbonate chemistry (Terhaar et al., 2022) as well as (b) the high-frequency variability of the ocean carbon sink anomalies as simulated by GOBMs that was derived after removing a spline fit to the simulated anomalies. The multi-model mean estimates are shown as blue lines and the multi-model standard deviation as blue shading. (c) The composite estimate is then the sum of the timeseries in (a) and (b). The uncertainties of the composite model-based estimates are the combined uncertainties of (a) and (b) plus the uncertainty from the spline fit (see Appendix for details). In addition, estimates from the GOBMs (olive line and shading for multi-model mean and standard deviation) and the  $p\text{CO}_2$  products from the

130

Global Carbon Budget 2023 (Friedlingstein et al., 2023) (orange lines and shading show the multi-product mean and standard deviations over 8  $p\text{CO}_2$  products from 1990 to 2022, brown lines show the shading for multi-product mean and standard deviation over 2  $p\text{CO}_2$  products from 1959 to 2021) are shown for comparison in (c) and the best estimate from the Global Carbon Budget 2023 (black line and shading for multi-model mean and uncertainty as reported in the Global Carbon Budget 2023) in (d).

135

## 2.2 Comparison to previous estimates of the global ocean carbon sink

The new composite model-based estimate of the global ocean carbon sink differs from previous estimates by  $p\text{CO}_2$  products and GOBMs in terms of magnitude, trend, and variability. The ocean carbon sink in the composite model-based estimate is 10% (11 Pg C) larger than the estimate from GOBMs for the period from 1959 to 2022 (Fig. A1a). The absolute difference 140 between both estimates has some variability over time but remains on average the same until 2014. After 2014, the composite estimate becomes steadily larger and the difference rises from 0.24 Pg C  $\text{yr}^{-1}$  (8%) averaged from 2005 to 2014 to 0.65 Pg C  $\text{yr}^{-1}$  (26%) in 2022 (Fig. A1a). The difference before 2014 is due to a bias in the GOBMs in their simulated circulation and carbonate chemistry (Terhaar et al., 2024) that also exists in ESMs but was corrected for (Terhaar et al., 2022) (Figure A1a). After 2014, the increasing difference may either be explained by slightly different trajectories of atmospheric CO<sub>2</sub> in ESMs 145 under SSP1-2.6 and the historical atmospheric CO<sub>2</sub>. Recently it has been shown that the trend in the ocean carbon sink is sensitively related to changes in the trend of atmospheric CO<sub>2</sub>. Based on this recently identified and quantified relationship between changes in the trend of atmospheric CO<sub>2</sub> and trends in the ocean carbon sink across ESMs (Terhaar, 2024) and the evolution of atmospheric CO<sub>2</sub> in the real world and in SSP1-2.6 after 2014, the trend of the ocean carbon sink in ESMs should 150 only have been 0.2 Pg C  $\text{yr}^{-1} \text{dec}^{-1}$  larger than in GOBMs and not 0.4 Pg C  $\text{yr}^{-1} \text{dec}^{-1}$  larger. The difference in the atmospheric CO<sub>2</sub> trajectory thus explains around half of the difference of both estimates after 2014. The other half might be the spin-up 155 strategy by GOBMs with too warm atmospheric during pre-industrial times that result in too weak transient ocean warming (Takano et al., 2023; Huguenin et al., 2022) and hence too little loss of natural carbon to the atmosphere as a consequence of this warming. However, to quantify such an effect, simulations with GOBMs following the spin-up strategy by Huguenin et al. (2022) would have to be performed.

155

Compared to  $p\text{CO}_2$  products, the composite estimate of the global ocean carbon sink is only 3% (1 Pg C) larger for the period from 1959 and 1989 than the two  $p\text{CO}_2$  products that provide estimates before 1990 and is 8% (7 Pg C) smaller than all 8  $p\text{CO}_2$  products on average for the period from 1990 to 2022 (Fig. A1b). The difference in the early 1990s and after 2000 might 160 be due to overly strong decadal variability that has been shown to exist at least in one  $p\text{CO}_2$  product (Gloege et al., 2021). This explanation is further supported by two further studies, one that showed that extrapolating unevenly spaced observations in space and time lead to overly strong trends in the estimates of the ocean carbon sink by  $p\text{CO}_2$  products (Hauck et al., 2023a) and one that used ESMs to show that the trends in  $p\text{CO}_2$  products lies outside of what can be expected based on changes in the atmospheric CO<sub>2</sub> growth rate and climate variability (Terhaar, 2024). After 2019, the difference between the composite model- 165

165 based estimate and the  $p\text{CO}_2$  products decreases again, likely because of the above discussed difference in observed atmospheric CO<sub>2</sub> and the prescribed atmospheric CO<sub>2</sub> in ESMs after 2014 following SSP1-2.6.

The composite estimate is almost identical to the best estimate of the ocean carbon sink provided by the Global Carbon Budget 2023 (Fig. 2d), which represents the average of the estimate by GOBMs and the  $p\text{CO}_2$  products, until the atmospheric CO<sub>2</sub> differs in the ESMs after 2015. The composite estimate thus corroborates this best estimate by the Global Carbon Budget 2023.

170 However, instead of simply averaging two independent estimates, the composite model-based estimate uses the best available knowledge to remove the weaknesses of each model-based estimate and to only keep the strengths. As the composite model-based estimate explains the differences, its uncertainty is around 70% smaller than that of the best estimate of the Global Carbon Budget 2023.

### 3 Conclusion

175 Overall, the composite model-based estimate of the global ocean carbon sink combines the strengths of two so far mostly separated model classes and successfully manages to account for the shortcomings in the different global ocean carbon sink estimates, i.e., the low bias in GOBMs due to the spin-up and the representation of the ocean circulation and carbonate chemistry and the bias towards too large decadal variability and trends in the  $p\text{CO}_2$  products. The same method could also be applied to derive composite model-based estimates of regional and monthly-resolved estimates of the ocean carbon sink.

180 Regionally composite estimates might, however, have larger uncertainties as differences in regional carbon sink estimates are often larger than global estimates (DeVries et al., 2023; Yasunaka et al., 2023; Hauck et al., 2023b; Perez et al., 2023; Terhaar et al., 2021c, 2022, 2021a, 2024), possibly due to a compensation of regional carbon fluxes, e.g., a low Southern Ocean carbon uptake can be compensated by a high North Atlantic Ocean carbon uptake.

185 Although this composite estimate provides an improvement to existing estimates of both model classes, GOBMs (Friedlingstein et al., 2023; DeVries et al., 2023) and ESMs (Terhaar et al., 2022), it still has shortcomings. One shortcoming is the forcing of ESMs with SSPs after 2014 that leads to slightly too high carbon sink estimates from 2015 to 2022. This shortcoming could be overcome if ESMs were run with observed atmospheric CO<sub>2</sub> after the historical forcing from CMIP6 ends in 2014. Another shortcoming is that all ESMs start in 1850 and are spun-up with atmospheric CO<sub>2</sub>, which leads of an 190 underestimation of the ocean carbon sink (Bronselaer et al., 2017) of around 0.05–0.10 Pg C yr<sup>-1</sup> for ESMs for the period from 1959 to 2022 (Terhaar et al., 2024). This underestimation could be removed if ESMs were to start before the industrial revolution and the associated increase in atmospheric CO<sub>2</sub>. Furthermore, the composite estimate cannot remove shortcomings or uncertainties that are inherent to both GOBMs and ESMs and that were not accounted for by emergent constraints (Terhaar et al., 2022), such as the often-incorrect representation of the seasonal cycle of  $p\text{CO}_2$  in both model classes (Rodgers et al., 195 2023; Joos et al., 2023). As it has been shown that the seasonal cycle changes in the future will affect the strength of the ocean

carbon sink by 8% until 2100 under a high-emission scenario (Fassbender et al., 2022), an incorrect representation at present likely also affects the simulated ocean carbon sink by ESMs and GOBMs and hence by the composite estimate. Other processes that are also still not at all or not accurately simulated in GOBMs and ESMs and that might affect the ocean carbon sink are, for example, the ocean biological carbon pump (Doney et al., 2024; Laufkötter et al., 2015) or the land-ocean aquatic continuum (Séférian et al., 2020; Terhaar et al., 2024). Although improvements have been made in the past to account for these model weaknesses (Dinauer et al., 2022; Archibald et al., 2019; Lacroix et al., 2020; Terhaar et al., 2021b), more research is needed to improve simulated estimates of the ocean carbon sink.

The need for a composite model-based estimate of the global ocean carbon arose due to shortcomings in both model classes.

As ESMs will always simulate an internal climate variability in a different phase than the observed one, this estimate remains a necessary fix until GOBMs are set up so that they can overcome their current weaknesses. To overcome current weaknesses, I recommend testing if an improved spin-up strategy that accounts for the difference in atmospheric and surface ocean temperatures as well as radiation between the pre-industrial times and the mid 20<sup>th</sup> century, for example as proposed by Huguenin et al. (2022), may explain differences in the trends of the ocean carbon sink between GOBMs and ESMs.

Furthermore, previous suggestions provided by Terhaar et al. (2024), such as a long enough spin-up and an early starting date and an associated atmospheric CO<sub>2</sub> during the spin-up, will likely also improve the carbon sink estimates by GOBMs. Once GOBMs are set-up in a common way, emergent constraints could also be used in GOBMs to correct for biases in the ocean circulation and carbonate chemistry as it was done for ESMs regionally and globally (Goris et al., 2018; Terhaar et al., 2021c, 2022, 2020; Bourgeois et al., 2022; Vaittinada Ayar et al., 2022). Until then, the here provided composite model-based estimate of the global ocean annually averaged carbon sink circumvents these shortcomings in GOBMs at present with the help of ESMs and thus provides a robust estimate of the global ocean carbon from 1959 to 2022.

## 4 Appendix

### 4.1 Estimates of the ocean carbon sink

220 Estimates of the ocean carbon sink, defined as the change in the globally integrated air-sea CO<sub>2</sub> flux since pre-industrial times due to increasing CO<sub>2</sub> and climate change, from *p*CO<sub>2</sub> products, GOBMs, and ESMs were used. Estimates of the global ocean carbon sink were directly taken for 8 *p*CO<sub>2</sub> products (Table A2) and 10 GOBMs (Table A3) from the Global Carbon Budget 2023 (Friedlingstein et al., 2023) (<https://doi.org/10.18160/gcp-2023>). In addition, the best estimate from the Global Carbon Budget 2023 was also directly taken from <https://doi.org/10.18160/gcp-2023>. For ESMs, estimates of the ocean carbon sink  
225 were calculated for 14 ESMs under historical forcing until 2014 and SSP1-2.6 from 2015 to 2022 following Terhaar et al. (2022) (Table A4).

The carbon sink estimates from ESMs were adjusted for biases in each model's circulation and carbonate chemistry as described by Terhaar et al (2022). Each model's annually averaged and globally integrated ocean carbon sink was adjusted based on three predictors that were previously identified to determine the strength of the ocean carbon sink. The rate by which  
230 surface water with high anthropogenic carbon is transported to the ocean interior and replaced by newly upwelled water was shown to be largely driven in ESMs by the surface ocean salinity in the Southern Ocean that largely determines the rate of formation of mode and intermediate waters in that region (Terhaar et al., 2021c) and the strength of the Atlantic Meridional Overturning Circulation that determines the strength of the subsurface water formation in the subpolar North Atlantic in ESMs (Terhaar et al., 2022). In addition, the globally averaged Revelle factor determines the amount of carbon that the surface ocean  
235 can take up for a given increase of CO<sub>2</sub> in the atmosphere in ESMs (Terhaar et al., 2022). These three predictors, the same as in Terhaar et al (2022), were used here. For the target variable, however, I here did not use the ocean carbon sink estimates from 1997 to 2014 but the ocean carbon sink from 1959 to 2022, the period for which this new composite model-based estimate provides annual ocean carbon sink estimates. To calculate the adjustment factors, I here used SSP5-8.5 after 2014 for which 3 more ESMs provide output (Table A4) as the higher number of ESMs makes the fit between predictors and target variables  
240 more robust (*r*<sup>2</sup> decreases from 0.82 to 0.63 when only using the 14 ESMs that provide output for SSP1-2.6). The adjustment increases the mean carbon sink in the ESMs and hence the estimate of the composite estimate by 11% and reduces the uncertainty by 12% (Fig. A2). Hence, the main part of the reduction in uncertainty stems indeed from the combination of the two model classes and not from the adjustment to the ESMs by Terhaar et al. (2022). However, the adjustment is necessary to adjust for a known bias in the strength of the ocean carbon sink in ESMs (Terhaar et al., 2022).

245 Instead of using several different ESMs, one could also have used large ensembles such as the GFDL-ESM2M large ensemble (Burger et al., 2022) or the CESM2 large ensemble (Rodgers et al., 2021). The advantage of such an ensemble with 30-50 ensemble members is indeed that the forced trend can be better isolated (Li and Ilyina, 2018). However, the disadvantage is that one model can have systematic biases in all its ensemble members. CESM2, for example, appears to have a strong low

bias in the Southern Ocean sea surface salinity, and hence the creation of mode and intermediate waters (Terhaar et al., 2021c).

250 The underestimation of the mode and intermediate water then leads to too little carbon uptake in the Southern Ocean, with a strong global imprint (see Figure 3 in (Terhaar et al., 2022)). The multi-model approach, on the other hand, has the distinct advantage that systematic biases in single models are averaged out to the best extent possible. Moreover, the use of these different models even allows to correct the multi-model estimate for biases that remain within the entire model ensemble (Terhaar et al., 2022). The disadvantage of the multi-model approach is that it has a smaller number of simulations so that the  
255 true forced trend may not be completely isolated, and some random variability may remain. However, as a spline fit is later fitted to the earth system model output, that variability is largely removed as well. Although not all internal variability might be filtered out entirely by the multi-model ensemble, I use this multi-model ensemble to avoid biases in the magnitude of the long-term carbon sink that could arise from using a large ensemble of a single model.

## 4.2 Separating high-frequency variability and long-term trends

260 The high-frequency variability and long-term trends of the annually averaged global carbon sink in ESMs and GOBMs were separated by fitting a spline following Enting (1987) to the respective ocean carbon sink estimate (Figs. A3 and A4). The fit itself represents the long-term trends and decadal variability and the residual, the difference between the original time series and the spline fit, is defined as the high-frequency variability. I here used an openly available python implementation of this spline fitting method ([https://github.com/friedrichs-repo/enting\\_spline](https://github.com/friedrichs-repo/enting_spline)) with a cut-off period of 15 years. The cut-off period  
265 describes the period where 50% of the signal is attenuated by the spline. 15 years was chosen to guarantee that all sub-decadal variability is removed from the original timeseries.

To test the sensitivity to the choice, a composite model-based estimate was also calculated using an 11-year running mean instead of an spline using Enting (1987) with a cut-off period of 15 years. The composite model-based estimate using the 11-

270 year running mean is almost indistinguishable from the estimate using Enting (1987) with a cut-off period of 15 years but differs at the start and the end of the timeseries (Fig. A5). The running mean flattens off at the ends of timeseries with strong trends because neither the smaller values before the beginning of the timeseries nor the potentially larger values after the end of the timeseries are included. Thus, I here decided to rely on the spline fit from Enting (1987).

275 The spline fit itself also comes with uncertainties due to the choice of the cutoff period. Here, I calculated the composite model-based estimate using cutoff periods from 10 to 20 years (Fig. A6). The resulting composite model-based estimate is insensitive to the choice of the cutoff period. This insensitivity shows that it is essential that the inter-annual variability is taken from the GOBMs and the long-term trends from the ESMs. The variability in between, however, can be taken from either GOBMs or ESMs as the decadal variability and trends of the ocean carbon sink are mainly driven by the change in the trends in atmospheric  
280 CO<sub>2</sub>, i.e., the growth rate of atmospheric CO<sub>2</sub>(McKinley et al., 2017, 2020; Fay et al., 2023; Terhaar, 2024), and other external

forcing such as volcanoes (McKinley et al., 2020; Fay et al., 2023; Frölicher et al., 2013), which are prescribed in GOBMs and ESMs (until 2014) based on observations. As GOBMs have external forcing, such as volcanoes, prescribed and ESMs have it prescribed until 2014, the end of the historical period in CMIP6, the long-term effect of volcanoes is part of the long-term ESM estimate and the short-term variability due to volcanoes is part of the short-term variability from GOBMs. As the same spline and cut-off period is used to separate long-term trend and short-term variability in GOBMs and ESMs, there is no double counting of the overall effect of volcanoes (Fay et al., 2023).

#### 4.3 Combining high-frequency variability and long-term trends to form the composite estimate

As described in the results, the composite estimate combines two components of the ocean carbon sink timeseries. One component is the short-term variability, and one component is the long-term trend. Mathematically, the ocean carbon sink can be separated into these two components:

$$\text{SOCEAN} = \text{SOCEAN}^{\text{STV}} + \text{SOCEAN}^{\text{LTT}}, \quad (1)$$

where  $\text{SOCEAN}$  is the total carbon sink and  $\text{SOCEAN}^{\text{STV}}$  is the short-term variability component and  $\text{SOCEAN}^{\text{LTT}}$  is the long-term trend component. The ocean carbon sink of each GOBM ( $\text{SOCEAN}^{\text{GOBM}}$ ) and each ESM ( $\text{SOCEAN}^{\text{ESM}}$ ) (after adjustment for biases) was then separated into their short-term variability components ( $\text{SOCEAN}^{\text{GOBM-STV}}$  and  $\text{SOCEAN}^{\text{ESM-STV}}$ ) and their long-term trend components ( $\text{SOCEAN}^{\text{GOBM-LTT}}$  and  $\text{SOCEAN}^{\text{ESM-LTT}}$ ):

$$\text{SOCEAN}^{\text{GOBM}} = \text{SOCEAN}^{\text{GOBM-STV}} + \text{SOCEAN}^{\text{GOBM-LTT}}, \quad (2)$$

$$\text{SOCEAN}^{\text{ESM}} = \text{SOCEAN}^{\text{ESM-STV}} + \text{SOCEAN}^{\text{ESM-LTT}}. \quad (3)$$

Here I performed the separation using an Enting spline with a 15 year cut-off period as described in section 4.2 and also tested the sensitivity of the results to a change in the cut-off period and to the use of a different method to extract the long-term trend, i.e., a running mean. The separation was performed for each model individually. If the same method is used to separate the short-term variability and the long-term trend ESMs and GOBMs, there is no double counting of forcing that is present in both ensembles, such as volcanoes (Fay et al., 2023).

As described in the Introduction and Results, the historic short-term variability is more accurately simulated in GOBMs as they are forced with atmospheric reanalysis data and the long-term trend is more accurately simulated in ESMs due different ways of setting up these GOBMs, e.g., the lengths of the spin-up, different atmospheric CO<sub>2</sub> during the pre-industrial spin-up (Terhaar et al., 2024), and a too warm pre-industrial ocean and hence too weak transient warming in GOBMs (Huguenin et al., 2022). Thus, the composite model-based estimate ( $\text{SOCEAN}^{\text{COMPOSITE}}$ ) is calculated as follows:

$$\text{SOCEAN}^{\text{COMPOSITE}} = \text{SOCEAN}^{\text{GOBM-STV}} + \text{SOCEAN}^{\text{ESM-LTT}}. \quad (4)$$

315

The ocean model components in the GOBM and ESM ensembles are not the same. Thus,  $\text{SOCEAN}^{\text{GOBM-STV}}$  and  $\text{SOCEAN}^{\text{ESM-LTT}}$  may be considered to be inconsistent. However, these two estimates do not need to be based on the same ocean model components, as there is no indication for a link between the long-term trend and short-term variability of the ocean carbon sink. Although it would be possible to only use the members of the GOBM and ESM ensembles that have an ocean model component that is used in an ESM and GOBM, I decided to use all available models in each ensemble as it allows to get the best available estimate of  $\text{SOCEAN}^{\text{GOBM-STV}}$  and  $\text{SOCEAN}^{\text{ESM-LTT}}$ .

320

#### 4.4 Uncertainty estimates

325

The uncertainties of the composite model-based estimate of the ocean carbon sink are a combination of the multi-model standard deviation of the high-frequency estimates from the GOBMs and the long-term trends from the ESMs, as well as the uncertainty from the choice of the cutoff period that was used to calculate the spline (Table A1). The uncertainty of the cutoff period was calculated as the standard deviation of all 11 estimates with cutoff periods from 10 to 20 years (Fig. A6). The different uncertainties are added using error propagation, i.e., by calculating the square root of the sums of the squares of each

330

uncertainty. The difference in the atmospheric CO<sub>2</sub> in the ESMs under SSP1-2.6 after 2014 was not explicitly added as an uncertainty but discussed as a caveat in the manuscript.

**Table A1: Annually averaged best estimates and uncertainties ( $1-\sigma$ ) of the global ocean carbon sink by the composite model-based estimate. All units are in Pg C yr $^{-1}$ .**

335

Year	Best estimate	Uncertainty from GOBMs	Uncertainty from ESMs	Uncertainty from	Combined uncertainty
				cutoff period	
1959	0.91	0.05	0.10	0.01	0.11
1960	0.85	0.08	0.08	0.01	0.11
1961	0.75	0.04	0.07	0.02	0.09
1962	0.83	0.04	0.07	0.02	0.08
1963	1.00	0.06	0.07	0.01	0.09
1964	1.09	0.05	0.07	0.01	0.09
1965	1.19	0.06	0.07	0.02	0.09
1966	1.11	0.06	0.07	0.02	0.10
1967	0.96	0.07	0.08	0.02	0.11
1968	1.07	0.05	0.09	0.02	0.10
1969	1.19	0.07	0.09	0.01	0.12
1970	1.04	0.11	0.09	0.00	0.14
1971	1.19	0.05	0.08	0.00	0.10
1972	1.52	0.12	0.08	0.01	0.14
1973	1.39	0.07	0.08	0.02	0.11
1974	1.35	0.06	0.08	0.02	0.11
1975	1.27	0.09	0.09	0.02	0.13
1976	1.47	0.06	0.10	0.02	0.12
1977	1.55	0.05	0.10	0.01	0.11
1978	1.56	0.05	0.10	0.00	0.11
1979	1.51	0.09	0.09	0.00	0.13
1980	1.75	0.07	0.08	0.01	0.11
1981	1.71	0.04	0.08	0.02	0.09
1982	1.89	0.07	0.07	0.03	0.11
1983	2.05	0.10	0.07	0.03	0.13
1984	1.84	0.10	0.08	0.01	0.13
1985	1.76	0.09	0.08	0.00	0.12
1986	1.85	0.07	0.08	0.02	0.11
1987	2.03	0.12	0.08	0.03	0.15
1988	1.85	0.12	0.08	0.03	0.14
1989	1.89	0.08	0.08	0.03	0.12
1990	1.97	0.05	0.08	0.02	0.09
1991	2.06	0.08	0.08	0.00	0.11
1992	2.27	0.06	0.08	0.01	0.10
1993	2.21	0.04	0.08	0.02	0.09
1994	1.96	0.07	0.08	0.03	0.11
1995	2.01	0.06	0.08	0.02	0.10

1996	2.02	0.05	0.09	0.02	0.10
1997	2.22	0.13	0.09	0.01	0.16
1998	2.29	0.13	0.09	0.00	0.16
1999	2.06	0.12	0.08	0.01	0.14
2000	2.03	0.10	0.08	0.02	0.13
2001	1.98	0.08	0.08	0.02	0.11
2002	2.40	0.04	0.08	0.01	0.09
2003	2.46	0.04	0.08	0.01	0.09
2004	2.40	0.04	0.08	0.01	0.09
2005	2.45	0.05	0.09	0.00	0.10
2006	2.55	0.04	0.10	0.01	0.10
2007	2.50	0.08	0.10	0.01	0.13
2008	2.50	0.07	0.10	0.01	0.13
2009	2.55	0.06	0.11	0.01	0.12
2010	2.50	0.04	0.11	0.01	0.12
2011	2.58	0.07	0.12	0.01	0.14
2012	2.65	0.06	0.13	0.01	0.15
2013	2.64	0.04	0.14	0.02	0.15
2014	2.79	0.04	0.15	0.03	0.16
2015	2.89	0.08	0.15	0.03	0.18
2016	2.94	0.08	0.16	0.02	0.18
2017	2.83	0.07	0.16	0.01	0.17
2018	2.96	0.05	0.15	0.00	0.16
2019	3.02	0.05	0.15	0.01	0.16
2020	3.07	0.08	0.14	0.01	0.16
2021	3.05	0.07	0.13	0.02	0.15
2022	3.11	0.03	0.14	0.02	0.14

**Table A2: Observation-based  $p\text{CO}_2$  products from the Global Carbon Budget 2023 (Friedlingstein et al., 2023).**

$p\text{CO}_2$ product	Time period in GCB 2023	References
CMEMS-LSCE-FFNNv2	1990-2022	(Chau et al., 2022)
JMA-MLR	1990-2022	(Iida et al., 2021)
LDEO-HPD	1959-2022	(Gloege et al., 2022; Bennington et al., 2022)
MPI-SOMFFN	1990-2022	(Landschützer et al., 2016)
NIES-ML3	1990-2022	(Zeng et al., 2022)
OS-ETHZ-GRaCER	1990-2022	(Gregor and Gruber, 2021)
Jena-MLS	1959-2022	(Rödenbeck et al., 2014, 2022)
UPEx-Watson	1990-2022	(Watson et al., 2020)

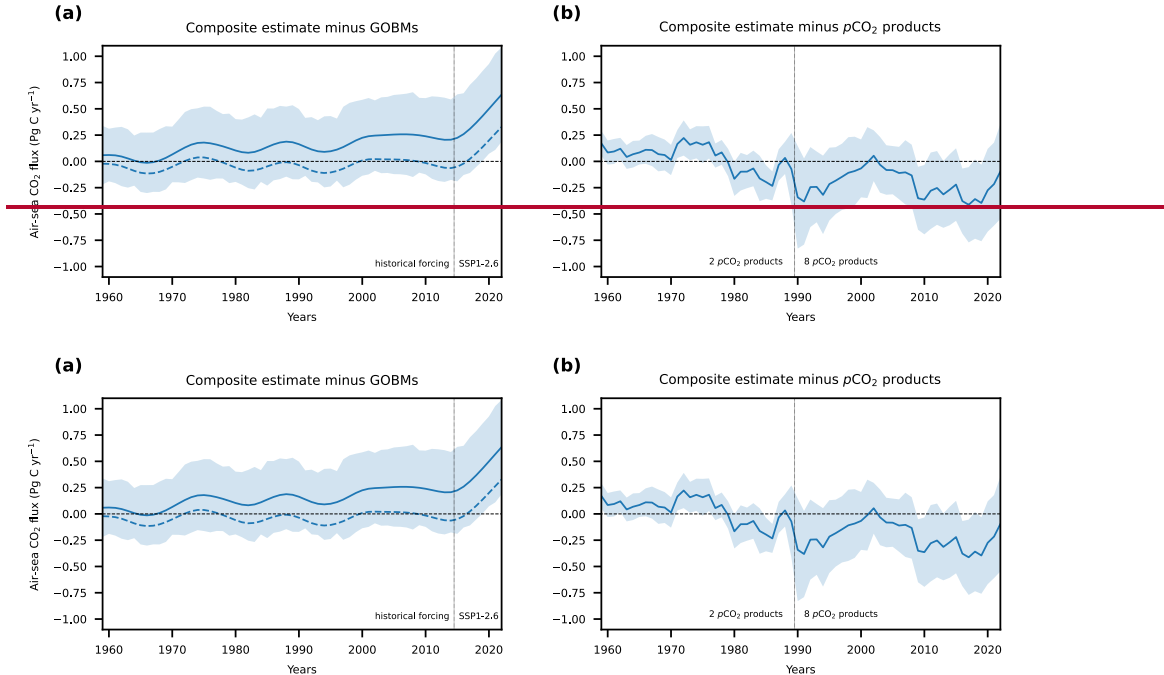
**Table A3: Global ocean biogeochemical models from the Global Carbon Budget 2023 (Friedlingstein et al., 2023).**

Model name	References
NEMO3.6-PISCESv2-gas (CNRM)	(Berhet et al., 2019; Séférian et al., 2019)
FESOM-2.1-REcoM2	(Gürses et al., 2023)
NEMO-PISCES (IPSL)	(Aumont et al., 2015)
MOM6-COBALT (Princeton)	(Liao et al., 2020)
MRI-ESM2-2	(Nakano et al., 2011; Urakawa et al., 2020)
MICOM-HAMOCC (NorESM-OCv1.2)	(Schwinger et al., 2016)
NEMO-PlankTOM12	(Wright et al., 2021)
CESM-ETHZ	(Doney et al., 2009)
MPIOM-HAMOCC6	(Lacroix et al., 2021a)
ACCESS (CSIRO)	(Law et al., 2017)

345

**Table A4: List of Earth System Models that were used in this study.**

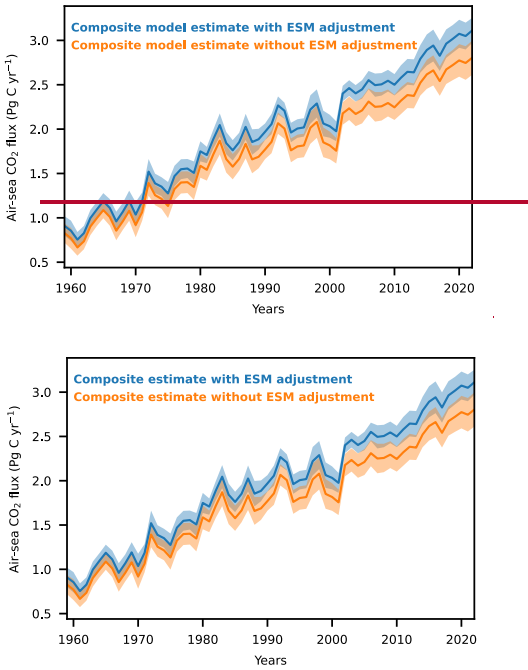
Model name	Available SSPs	References
ACCESS-ESM1-5	SSP1-2.6 / SSP5-8.5	(Ziehn et al., 2020)
CanESM5	SSP1-2.6 / SSP5-8.5	(Swart et al., 2019; Christian et al., 2022)
CanESM5-CanOE	SSP1-2.6 / SSP5-8.5	(Swart et al., 2019; Christian et al., 2022)
CESM2	SSP1-2.6 / SSP5-8.5	(Danabasoglu et al., 2020)
CESM2-WACCM	SSP1-2.6 / SSP5-8.5	(Danabasoglu et al., 2020)
CMCC-ESM2	SSP1-2.6 / SSP5-8.5	(Lovato et al., 2022)
EC-Earth3-CC	SSP5-8.5	(Döscher et al., 2022)
GFDL-CM4	SSP5-8.5	(Held et al., 2019)
GFDL-ESM4	SSP1-2.6 / SSP5-8.5	(Dunne et al., 2020; Stock et al., 2020)
IPSL-CM6A-LR	SSP1-2.6 / SSP5-8.5	(Boucher et al., 2020)
MIROC-ES2L	SSP1-2.6 / SSP5-8.5	(Hajima et al., 2020)
MPI-ESM1-2-HR	SSP1-2.6 / SSP5-8.5	(Gutjahr et al., 2019)
MPI-ESM1-2-LR	SSP1-2.6 / SSP5-8.5	(Mauritsen et al., 2019)
MRI-ESM2-0	SSP5-8.5	(Yukimoto et al., 2019)
NorESM2-LM	SSP1-2.6 / SSP5-8.5	(Tjiputra et al., 2020; Selander et al., 2020)
NorESM2-MM	SSP1-2.6 / SSP5-8.5	(Tjiputra et al., 2020; Selander et al., 2020)
UKESM1-0-LL	SSP1-2.6 / SSP5-8.5	(Sellier et al., 2020)



**Figure A1: Difference in estimates of the global ocean carbon sink between the new composite estimate and estimates from GOBMs and  $p\text{CO}_2$  products.** Difference between the composite estimate of the global ocean carbon sink and the estimates (a) from GOBMs and (b)  $p\text{CO}_2$  products from the Global Carbon Budget 2023 (Friedlingstein et al., 2023). The solid blue lines indicate the mean difference and the uncertainties show the combined uncertainties from the two respective estimates. The dashed line in (a) shows the difference between the composite estimate and the GOBMs when the ESMs are not adjusted before.

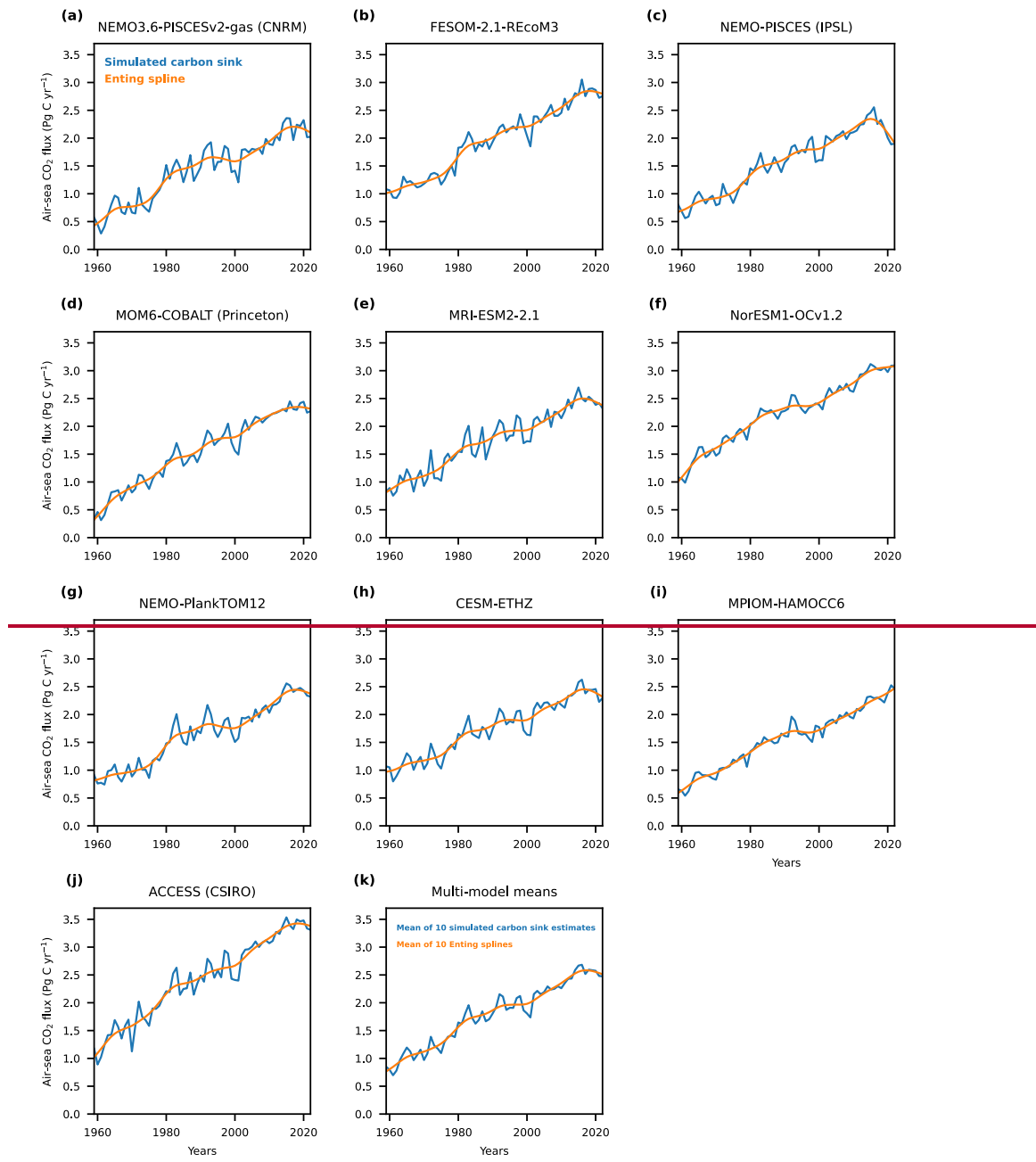
350

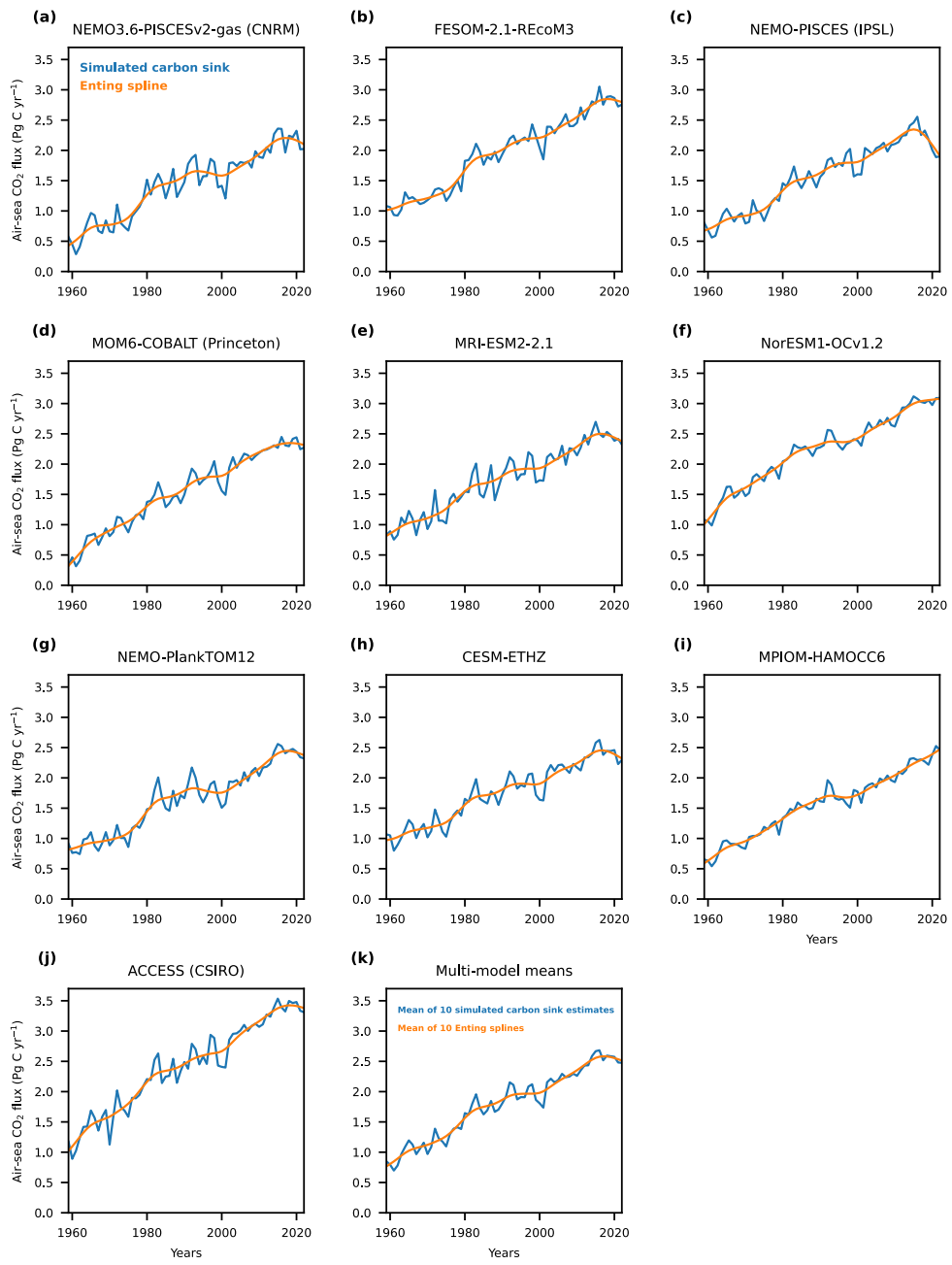
355



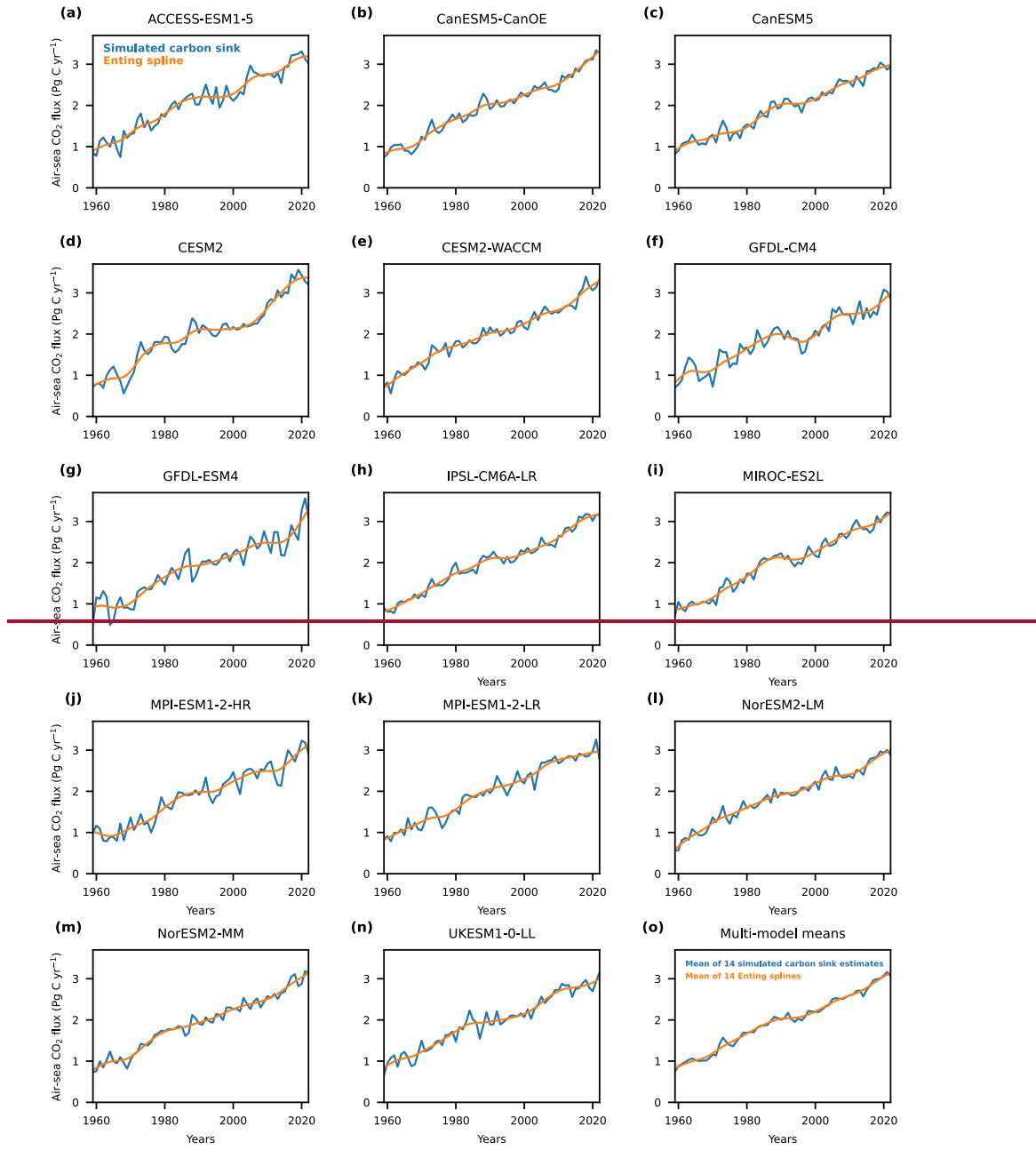
**Figure A2: Difference in the composite model-based estimates with and without the adjustment for biases in the ocean carbon sink in earth system models due to the circulation and surface ocean carbonate chemistry.** The composite estimate is shown with the adjustment by Terhaar et al. (2022) (blue line) and without the adjustment (orange line).

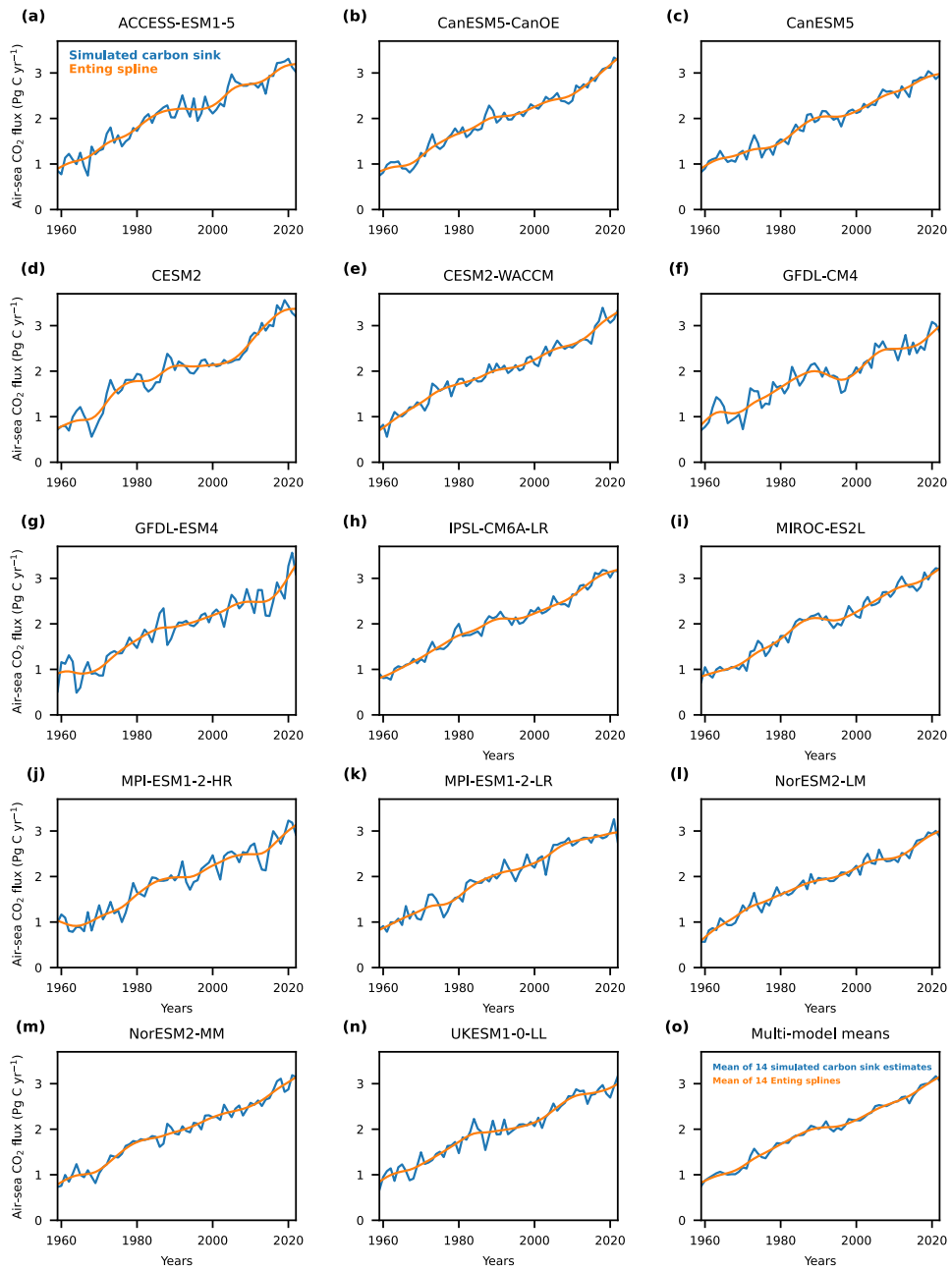
360



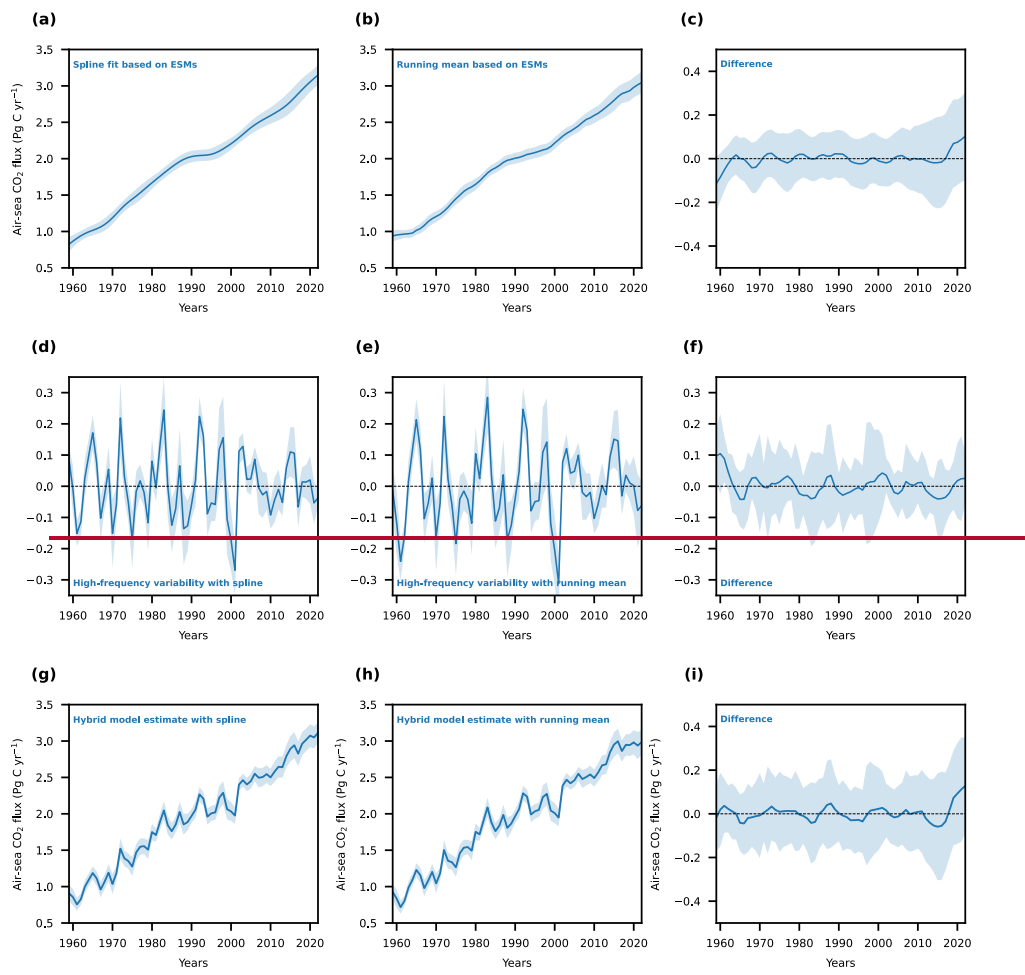


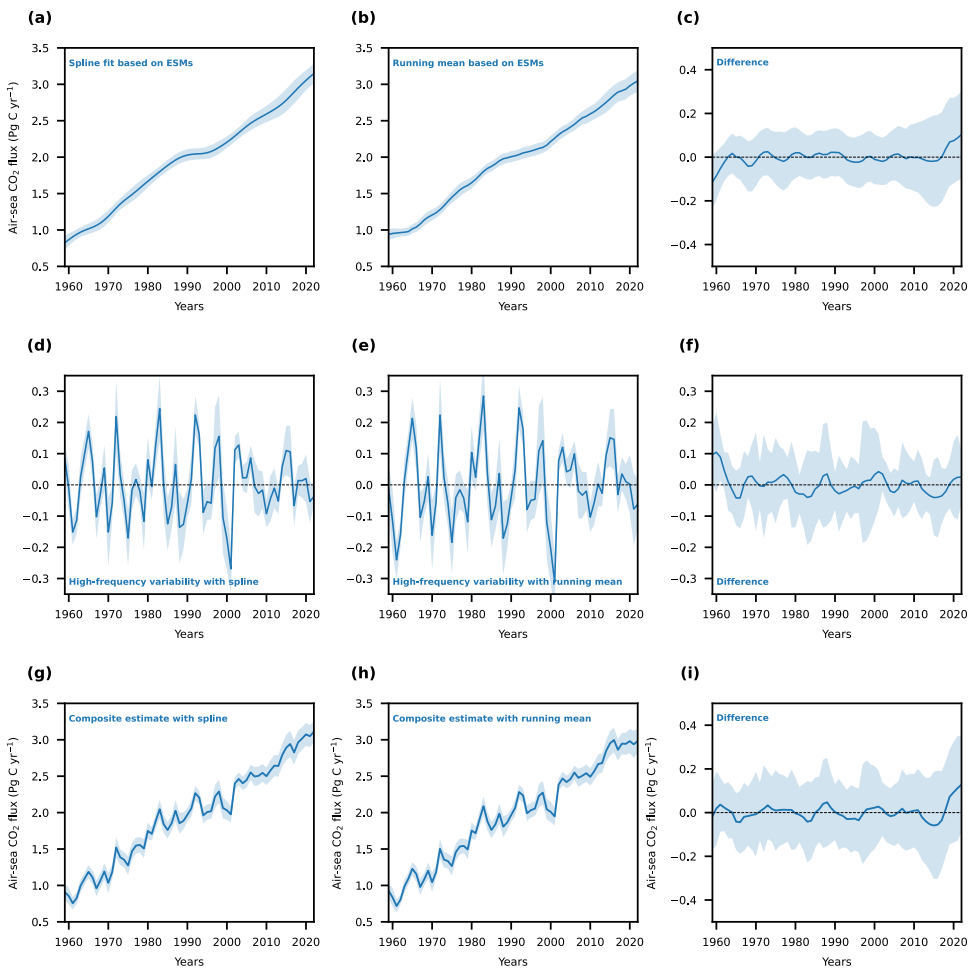
**Figure A3: The annual ocean carbon sink as simulated by 10 global ocean biogeochemistry models with an Enting spline fit using a 15 year cut-off period. (a) – (j) The simulated annual ocean carbon sink for 10 models from the Global Carbon Budget 2023 (Friedlingstein et al., 2023) and the (k) multi-model average (blue lines). An Enting spline fit to each simulated carbon sink and the mean of all spline fits are shown as orange lines.**





**Figure A4: The annual ocean carbon sink as simulated by 14 earth system models and adjusted for biases in circulation and surface ocean carbon chemistry with an Enting spline fit using a 15 year cut-off period. (a) – (n)** The simulated annual ocean carbon sink for 14 models that were adjusted for biases in the circulation and surface ocean carbon chemistry and the (k) multi-model average (blue lines). An Enting spline fit to each simulated carbon sink and the mean of all spline fits are shown as orange lines.





380

**Figure A5: Difference in estimates of the global ocean carbon sink between the new composite estimate and estimates from GOBMs and pCO<sub>2</sub> products.** Difference between the composite estimate of the global ocean carbon sink and the estimates (a) from GOBMs and (b) pCO<sub>2</sub> products from the Global Carbon Budget 2023 (Friedlingstein et al., 2023). The blue lines indicate the mean difference and the uncertainties show the combined uncertainties from the two respective estimates.

385

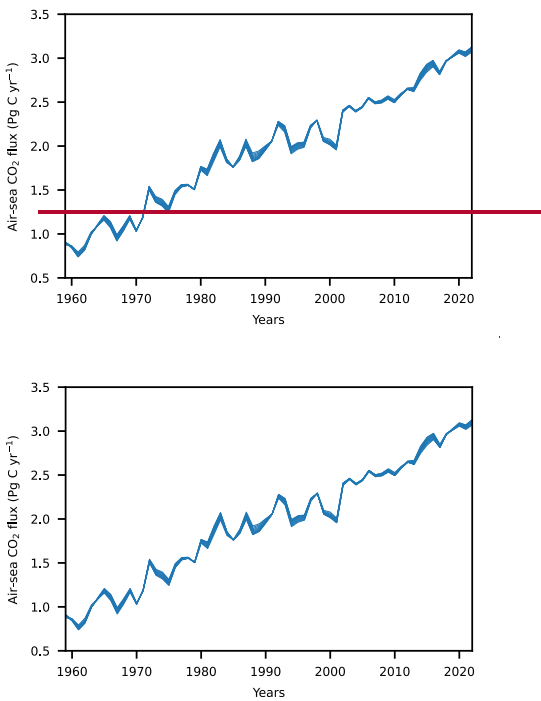


**Figure A6: The global ocean carbon sink estimate by the composite model-based estimate using different cutoff periods.** Each of the 11 lines here represents the global ocean carbon sink estimate by the composite model-based estimate using cutoff periods from 10 to 20 years.

390

395 **Data availability**

The Earth system model output used in this study is available via the Earth System Grid Federation (<https://esgf-node.ipsl.upmc.fr/projects/esgf-ipsl/>, last access: 1 June 2022). The data from the Global Carbon Budget 2023 is available here (<https://doi.org/10.18160/gcp-2023>). The best estimate and uncertainties of the annually averaged estimate of the global carbon sink provided as estimated by the here presented composite model-based estimate are presented in table A1. If composite model-based estimate is too long for tables in other studies, please reference it as GOBM-ESM estimate.

400

**Competing interests**

The author has declared that he has no competing interests.

**Acknowledgments**

I thank Thomas L. Frölicher for helpful comments on the manuscript and the Swiss National Science Foundation for funding  
405 under grant # PZ00P2\_209044 (ArcticECO).

## References

- Archibald, K. M., Siegel, D. A., and Doney, S. C.: Modeling the Impact of Zooplankton Diel Vertical Migration on the Carbon  
410 Export Flux of the Biological Pump, Global Biogeochem. Cycles, 33, 181–199,  
<https://doi.org/https://doi.org/10.1029/2018GB005983>, 2019.
- Aumont, O., Ethé, C., Tagliabue, A., Bopp, L., and Gehlen, M.: PISCES-v2: an ocean biogeochemical model for carbon and  
ecosystem studies, Geosci. Model Dev., 8, 2465–2513, <https://doi.org/10.5194/gmd-8-2465-2015>, 2015.  
415
- Bennington, V., Gloege, L., and McKinley, G. A.: Observation-based variability in the global ocean carbon sink from 1959–  
2020, Earth Sp. Sci. Open Arch., 14, <https://doi.org/10.1002/essoar.10510815.1>, 2022.
- Berthet, S., Séferian, R., Bricaud, C., Chevallier, M., Voldoire, A., and Ethé, C.: Evaluation of an Online Grid-Coarsening  
420 Algorithm in a Global Eddy-Admitting Ocean Biogeochemical Model, J. Adv. Model. Earth Syst., 11, 1759–1783,  
<https://doi.org/https://doi.org/10.1029/2019MS001644>, 2019.
- Boucher, O., Servonnat, J., Albright, A. L., Aumont, O., Balkanski, Y., Bastrikov, V., Bekki, S., Bonnet, R., Bony, S., Bopp,  
L., Braconnot, P., Brockmann, P., Cadule, P., Caubel, A., Cheruy, F., Codron, F., Cozic, A., Cugnet, D., D'Andrea, F., Davini,  
425 P., de Lavergne, C., Denvil, S., Deshayes, J., Devilliers, M., Ducharne, A., Dufresne, J.-L., Dupont, E., Éthé, C., Fairhead, L.,  
Falletti, L., Flavoni, S., Foujols, M.-A., Gardoll, S., Gastineau, G., Ghattas, J., Grandpeix, J.-Y., Guenet, B., Guez E., L.,  
Guilyardi, E., Guimberteau, M., Hauglustaine, D., Hourdin, F., Idelkadi, A., Joussaume, S., Kageyama, M., Khodri, M.,  
Krinner, G., Lebas, N., Levavasseur, G., Lévy, C., Li, L., Lott, F., Lurton, T., Luyssaert, S., Madec, G., Madeleine, J.-B.,  
Maignan, F., Marchand, M., Marti, O., Mellul, L., Meurdesoif, Y., Mignot, J., Musat, I., Ottlé, C., Peylin, P., Planton, Y.,  
430 Polcher, J., Rio, C., Rochetin, N., Rousset, C., Sepulchre, P., Sima, A., Swingedouw, D., Thiéblemont, R., Traore, A. K.,  
Vancoppenolle, M., Vial, J., Vialard, J., Viovy, N., and Vuichard, N.: Presentation and Evaluation of the IPSL-CM6A-LR  
Climate Model, J. Adv. Model. Earth Syst., 12, e2019MS002010, <https://doi.org/https://doi.org/10.1029/2019MS002010>,  
2020.
- Bourgeois, T., Goris, N., Schwinger, J., and Tjiputra, J. F.: Stratification constrains future heat and carbon uptake in the  
435 Southern Ocean between 30°S and 55°S, Nat. Commun., 13, 340, <https://doi.org/10.1038/s41467-022-27979-5>, 2022.
- Broecker, W. S., TTakahashi, T., Simpson, H. J., and Peng T.-H.: Fate of Fossil Fuel Carbon Dioxide and the Global Carbon  
Budget, Science, 206, 409–418, <https://doi.org/10.1126/science.206.4417.409>, 1979.  
440

Bronselaer, B., Winton, M., Russell, J., Sabine, C. L., and Khatiwala, S.: Agreement of CMIP5 Simulated and Observed Ocean Anthropogenic CO<sub>2</sub> Uptake, Geophys. Res. Lett., 44, 12, 212–298, 305, <https://doi.org/https://doi.org/10.1002/2017GL074435>, 2017.

445 Burger, F. A., Terhaar, J., and Frölicher, T. L.: Compound marine heatwaves and ocean acidity extremes, Nat. Commun., 13, 4722, <https://doi.org/10.1038/s41467-022-32120-7>, 2022.

Chau, T. T. T., Gehlen, M., and Chevallier, F.: A seamless ensemble-based reconstruction of surface ocean pCO<sub>2</sub> and air-sea CO<sub>2</sub> fluxes over the global coastal and open oceans, 19, 1087–1109, <https://doi.org/10.5194/bg-19-1087-2022>, 2022.

450 Christian, J. R., Denman, K. L., Hayashida, H., Holdsworth, A. M., Lee, W. G., Riche, O. G. J., Shao, A. E., Steiner, N., and Swart, N. C.: Ocean biogeochemistry in the Canadian Earth System Model version 5.0.3: CanESM5 and CanESM5-CanOE, Geosci. Model Dev., 15, 4393–4424, <https://doi.org/10.5194/gmd-15-4393-2022>, 2022.

Danabasoglu, G., Lamarque, J.-F., Bacmeister, J., Bailey, D. A., DuVivier, A. K., Edwards, J., Emmons, L. K., Fasullo, J.,  
455 Garcia, R., Gettelman, A., Hannay, C., Holland, M. M., Large, W. G., Lauritzen, P. H., Lawrence, D. M., Lenaerts, J. T. M.,  
Lindsay, K., Lipscomb, W. H., Mills, M. J., Neale, R., Oleson, K. W., Otto-Btiesner, B., Phillips, A. S., Sacks, W., Tilmes, S.,  
van Kampenhout, L., Vertenstein, M., Bertini, A., Dennis, J., Deser, C., Fischer, C., Fox-Kemper, B., Kay, J. E., Kinnison, D.,  
Kushner, P. J., Larson, V. E., Long, M. C., Mickelson, S., Moore, J. K., Nienhouse, E., Polvani, L., Rasch, P. J., and Strand,  
460 W. G.: The Community Earth System Model Version 2 (CESM2), J. Adv. Model. Earth Syst., 12,  
<https://doi.org/https://doi.org/10.1029/2019MS001916>, 2020.

DeVries, T., Yamamoto, K., Wanninkhof, R., Gruber, N., Hauck, J., Müller, J. D., Bopp, L., Carroll, D., Carter, B. R., Chau,  
T. T. T., Doney, S. C., Gehlen, M., Gloege, L., Gregor, L., Henson, S., Kim, J. H., Iida, Y., Ilyina, T., Landschützer, P., Le  
Quéré, C., Munro, D. R., Nissen, C., Patara, L., Perez, F. F., Resplandy, L., Rodgers, K. B., Schwinger, J., Séférian, R., Sicardi,  
465 V., Terhaar, J., Triñanes, J., Tsujino, H., Watson, A. J., Yasunaka, S., and Zeng, J.: Magnitude, trends, and variability of the  
global ocean carbon sink from 1985–2018, Global Biogeochem. Cycles, 2023.

Dinauer, A., Laufkötter, C., Doney, S. C., and Joos, F.: What Controls the Large-Scale Efficiency of Carbon Transfer Through  
the Ocean’s Mesopelagic Zone? Insights From a New, Mechanistic Model (MSPACMAM), Global Biogeochem. Cycles, 36,  
470 e2021GB007131, <https://doi.org/https://doi.org/10.1029/2021GB007131>, 2022.

Doney, S. C., Lima, I., Feely, R. A., Glover, D. M., Lindsay, K., Mahowald, N., Moore, J. K., and Wanninkhof, R.: Mechanisms governing interannual variability in upper-ocean inorganic carbon system and air-sea CO<sub>2</sub> fluxes: Physical  
climate and atmospheric dust, Deep Sea Res. Part II Top. Stud. Oceanogr., 56, 640–655,

475 https://doi.org/https://doi.org/10.1016/j.dsr2.2008.12.006, 2009.

Doney, S. C., Mitchell, K. A., Henson, S. A., Cavan, E., DeVries, T., Gruber, N., Hauck, J., Mouw, C. B., Müller, J. D., and Primeau, F. W.: Observational and Numerical Modeling Constraints on the Global Ocean Biological Carbon Pump, *Global Biogeochem. Cycles*, 38, e2024GB008156, <https://doi.org/https://doi.org/10.1029/2024GB008156>, 2024.

480

Döscher, R., Acosta, M., Alessandri, A., Anthoni, P., Arsouze, T., Bergman, T., Bernardello, R., Boussetta, S., Caron, L.-P., Carver, G., Castrillo, M., Catalano, F., Cvijanovic, I., Davini, P., Dekker, E., Doblas-Reyes, F. J., Docquier, D., Echevarria, P., Fladrich, U., Fuentes-Franco, R., Gröger, M., v. Hardenberg, J., Hieronymus, J., Karami, M. P., Keskinen, J.-P., Koenigk, T., Makkonen, R., Massonnet, F., Ménégoz, M., Miller, P. A., Moreno-Chamarro, E., Nieradzik, L., van Noije, T., Nolan, P., 485 O'Donnell, D., Ollinaho, P., van den Oord, G., Ortega, P., Prims, O. T., Ramos, A., Reerink, T., Rousset, C., Ruprich-Robert, Y., Le Sager, P., Schmitt, T., Schrödner, R., Serva, F., Sicardi, V., Sloth Madsen, M., Smith, B., Tian, T., Tourigny, E., Uotila, P., Vancoppenolle, M., Wang, S., Wårlind, D., Willén, U., Wyser, K., Yang, S., Yepes-Arbós, X., and Zhang, Q.: The EC-Earth3 Earth system model for the Coupled Model Intercomparison Project 6, *Geosci. Model Dev.*, 15, 2973–3020, <https://doi.org/10.5194/gmd-15-2973-2022>, 2022.

490

Dunne, J. P., Horowitz, L. W., Adcroft, A. J., Ginoux, P., Held, I. M., John, J. G., Krasting, J. P., Malyshev, S., Naik, V., Paulot, F., Shevliakova, E., Stock, C. A., Zadeh, N., Balaji, V., Blanton, C., Dunne, K. A., Dupuis, C., Durachta, J., Dussin, R., Gauthier, P. P. G., Griffies, S. M., Guo, H., Hallberg, R. W., Harrison, M., He, J., Hurlin, W., McHugh, C., Menzel, R., Milly, P. C. D., Nikonorov, S., Paynter, D. J., Poshay, J., Radhakrishnan, A., Rand, K., Reichl, B. G., Robinson, T., 495 Schwarzkopf, D. M., Sentman, L. T., Underwood, S., Vahlenkamp, H., Winton, M., Wittenberg, A. T., Wyman, B., Zeng, Y., and Zhao, M.: The GFDL Earth System Model Version 4.1 (GFDL-ESM 4.1): Overall Coupled Model Description and Simulation Characteristics, *J. Adv. Model. Earth Syst.*, 12, e2019MS002015, <https://doi.org/https://doi.org/10.1029/2019MS002015>, 2020.

500

Enting, I. G.: On the use of smoothing splines to filter CO<sub>2</sub> data, *J. Geophys. Res. Atmos.*, 92, 10977–10984, <https://doi.org/https://doi.org/10.1029/JD092iD09p10977>, 1987.

505

Fassbender, A. J., Schlunegger, S., Rodgers, K. B., and Dunne, J. P.: Quantifying the Role of Seasonality in the Marine Carbon Cycle Feedback: An ESM2M Case Study, *Global Biogeochem. Cycles*, 36, e2021GB007018, <https://doi.org/https://doi.org/10.1029/2021GB007018>, 2022.

Fay, A. R., Gregor, L., Landschützer, P., McKinley, G. A., Gruber, N., Gehlen, M., Iida, Y., Laruelle, G. G., Rödenbeck, C., Roobaert, A., and Zeng, J.: SeaFlux: harmonization of air-sea CO<sub>2</sub> fluxes from surface pCO<sub>2</sub> data products using a standardized

510

Fay, A. R., McKinley, G. A., Lovenduski, N. S., Eddebar, Y., Levy, M. N., Long, M. C., Olivarez, H. C., and Rustagi, R. R.: Immediate and long-lasting impacts of the Mt. Pinatubo eruption on ocean oxygen and carbon inventories, *Global Biogeochem. Cycles*, n/a, e2022GB007513, [https://doi.org/https://doi.org/10.1029/2022GB007513](https://doi.org/10.1029/2022GB007513), 2023.

515 Friedlingstein, P., O’Sullivan, M., Jones, M. W., Andrew, R. M., Bakker, D. C. E., Hauck, J., Landschützer, P., Le Quéré, C., Luijckx, I. T., Peters, G. P., Peters, W., Pongratz, J., Schwingshakl, C., Sitch, S., Canadell, J. G., Ciais, P., Jackson, R. B., Alin, S. R., Anthoni, P., Barbero, L., Bates, N. R., Becker, M., Bellouin, N., Decharme, B., Bopp, L., Brasika, I. B. M., Cadule, P., Chamberlain, M. A., Chandra, N., Chau, T.-T.-T., Chevallier, F., Chini, L. P., Cronin, M., Dou, X., Enyo, K., Evans, W., Falk, S., Feely, R. A., Feng, L., Ford, D. J., Gasser, T., Ghattas, J., Gkritzalis, T., Grassi, G., Gregor, L., Gruber, N., Gürses, Ö., Harris, I., Hefner, M., Heinke, J., Houghton, R. A., Hurt, G. C., Iida, Y., Ilyina, T., Jacobson, A. R., Jain, A., Jarníková, T., Jersild, A., Jiang, F., Jin, Z., Joos, F., Kato, E., Keeling, R. F., Kennedy, D., Klein Goldewijk, K., Knauer, J., Korsbakken, J. I., Kötzinger, A., Lan, X., Lefèvre, N., Li, H., Liu, J., Liu, Z., Ma, L., Marland, G., Mayot, N., McGuire, P. C., McKinley, G. A., Meyer, G., Morgan, E. J., Munro, D. R., Nakaoka, S.-I., Niwa, Y., O’Brien, K. M., Olsen, A., Omar, A. M., Ono, T., Paulsen, M., Pierrot, D., Pocock, K., Poulter, B., Powis, C. M., Rehder, G., Resplandy, L., Robertson, E., Rödenbeck, C., 520 Rosan, T. M., Schwinger, J., Séférian, R., et al.: Global Carbon Budget 2023, *Earth Syst. Sci. Data*, 15, 5301–5369, <https://doi.org/10.5194/essd-15-5301-2023>, 2023.

525 Frölicher, T. L., Joos, F., Raible, C. C., and Sarmiento, J. L.: Atmospheric CO<sub>2</sub> response to volcanic eruptions: The role of ENSO, season, and variability, *Global Biogeochem. Cycles*, 27, 239–251, <https://doi.org/https://doi.org/10.1002/gbc.20028>, 530 2013.

Gloegel, L., McKinley, G. A., Landschützer, P., Fay, A. R., Frölicher, T. L., Fyfe, J. C., Ilyina, T., Jones, S., Lovenduski, N. S., Rodgers, K. B., Schlunegger, S., and Takano, Y.: Quantifying Errors in Observationally Based Estimates of Ocean Carbon Sink Variability, *Global Biogeochem. Cycles*, 35, e2020GB006788, <https://doi.org/https://doi.org/10.1029/2020GB006788>, 535 2021.

Gloegel, L., Yan, M., Zheng, T., and McKinley, G. A.: Improved Quantification of Ocean Carbon Uptake by Using Machine Learning to Merge Global Models and pCO<sub>2</sub> Data, *J. Adv. Model. Earth Syst.*, 14, e2021MS002620, <https://doi.org/https://doi.org/10.1029/2021MS002620>, 2022.

540

Goris, N., Tjiputra, J. F., Olsen, A., Schwinger, J., Lauvset, S. K., and Jeansson, E.: Constraining Projection-Based Estimates of the Future North Atlantic Carbon Uptake, *J. Clim.*, 31, 3959–3978, <https://doi.org/10.1175/JCLI-D-17-0564.1>, 2018.

Gregor, L. and Gruber, N.: OceanSODA-ETHZ: a global gridded data set of the surface ocean carbonate system for seasonal  
545 to decadal studies of ocean acidification, *Earth Syst. Sci. Data*, 13, 777–808, <https://doi.org/10.5194/essd-13-777-2021>, 2021.

Gregor, L., Lebehot, A. D., Kok, S., and Scheel Monteiro, P. M.: A comparative assessment of the uncertainties of global  
550 surface ocean CO<sub>2</sub> estimates using a machine-learning ensemble (CSIR-ML6 version2019a) – have we hit the wall?, *Geosci.  
Model Dev.*, 12, 5113–5136, <https://doi.org/10.5194/gmd-12-5113-2019>, 2019.

Gürses, Ö., Oziel, L., Karakus, O., Sidorenko, D., Völker, C., Ye, Y., Zeising, M., and Hauck, J.: Ocean biogeochemistry in  
555 the coupled ocean-sea ice-biogeochemistry model FESOM2.1-REcoM3, *Geosci. Model Dev. Discuss.*, 2023, 1–73,  
<https://doi.org/10.5194/gmd-2023-2>, 2023.

555 Gutjahr, O., Putrasahan, D., Lohmann, K., Jungclaus, J. H., von Storch, J.-S., Brüggemann, N., Haak, H., and Stössel, A.: Max  
Planck Institute Earth System Model (MPI-ESM1.2) for the High-Resolution Model Intercomparison Project (HighResMIP),  
*Geosci. Model Dev.*, 12, 3241–3281, <https://doi.org/10.5194/gmd-12-3241-2019>, 2019.

Hajima, T., Watanabe, M., Yamamoto, A., Tatebe, H., Noguchi, M. A., Abe, M., Ohgaito, R., Ito, A., Yamazaki, D., Okajima,  
560 H., Ito, A., Takata, K., Ogochi, K., Watanabe, S., and Kawamiya, M.: Development of the MIROC-ES2L Earth system model  
and the evaluationof biogeochemical processes and feedbacks, *Geosci. Model Dev.*, 13, 2197–2244,  
<https://doi.org/10.5194/gmd-13-2197-2020>, 2020.

Hauck, J., Nissen, C., Landschützer, P., Rödenbeck, C., Bushinsky, S., and Olsen, A.: Sparse observations induce large biases  
565 in estimates of the global ocean CO<sub>2</sub> sink: an ocean model subsampling experiment, *Philos. Trans. R. Soc. A Math. Phys. Eng.  
Sci.*, 381, 20220063, <https://doi.org/10.1098/rsta.2022.0063>, 2023a.

Hauck, J., Gregor, L., Nissen, C., Patara, L., Hague, M., Mongwe, N. P., Bushinsky, S. M., Doney, S. C., Gruber, N., Le Quéré,  
570 C., Manizza, M., Mazloff, M. R., Monteiro, P. M. S., and Terhaar, J.: The Southern Ocean carbon cycle 1985-2018: mean,  
seasonal cycle, trends and storage, *Global Biogeochem. Cycles*, 2023b.

Held, I. M., Guo, H., Adcroft, A., Dunne, J. P., Horowitz, L. W., Krasting, J., Shevliakova, E., Winton, M., Zhao, M., Bushuk,  
575 M., Wittenberg, A. T., Wyman, B., Xiang, B., Zhang, R., Anderson, W., Balaji, V., Donner, L., Dunne, K., Durachta, J.,  
Gauthier, P. P. G., Ginoux, P., Golaz, J.-C., Griffies, S. M., Hallberg, R., Harris, L., Harrison, M., Hurlin, W., John, J., Lin,  
P., Lin, S.-J., Malyshev, S., Menzel, R., Milly, P. C. D., Ming, Y., Naik, V., Paynter, D., Paulot, F., Ramaswamy, V., Reichl,  
B., Robinson, T., Rosati, A., Seman, C., Silvers, L. G., Underwood, S., and Zadeh, N.: Structure and Performance of GFDL's

CM4.0 Climate Model, J. Adv. Model. Earth Syst., 11, 3691–3727, <https://doi.org/https://doi.org/10.1029/2019MS001829>, 2019.

580 Hersbach, H., Bell, B., Berrisford, P., Hirahara, S., Horányi, A., Muñoz-Sabater, J., Nicolas, J., Peubey, C., Radu, R., Schepers, D., Simmons, A., Soci, C., Abdalla, S., Abellán, X., Balsamo, G., Bechtold, P., Biavati, G., Bidlot, J., Bonavita, M., De Chiara, G., Dahlgren, P., Dee, D., Diamantakis, M., Dragani, R., Flemming, J., Forbes, R., Fuentes, M., Geer, A., Haimberger, L., Healy, S., Hogan, R. J., Hólm, E., Janisková, M., Keeley, S., Laloyaux, P., Lopez, P., Lupu, C., Radnoti, G., de Rosnay, P., Rozum, I., Vamborg, F., Villaume, S., and Thépaut, J.-N.: The ERA5 global reanalysis, Q. J. R. Meteorol. Soc., 146, 1999–  
585 2049, <https://doi.org/https://doi.org/10.1002/qj.3803>, 2020.

Huguenin, M. F., Holmes, R. M., and England, M. H.: Drivers and distribution of global ocean heat uptake over the last half century, Nat. Commun., 13, 4921, <https://doi.org/10.1038/s41467-022-32540-5>, 2022.

590 Iida, Y., Takatani, Y., Kojima, A., and Ishii, M.: Global trends of ocean CO<sub>2</sub> sink and ocean acidification: an observation-based reconstruction of surface ocean inorganic carbon variables, J. Oceanogr., 77, 323–358, <https://doi.org/10.1007/s10872-020-00571-5>, 2021.

595 Joos, F., Hameau, A., Frölicher, T. L., and Stephenson, D. B.: Anthropogenic Attribution of the Increasing Seasonal Amplitude in Surface Ocean pCO<sub>2</sub>, Geophys. Res. Lett., 50, e2023GL102857, <https://doi.org/https://doi.org/10.1029/2023GL102857>, 2023.

600 Kanamitsu, M., Ebisuzaki, W., Woollen, J., Yang, S.-K., Hnilo, J. J., Fiorino, M., and Potter, G. L.: NCEP–DOE AMIP-II Reanalysis (R-2), Bull. Am. Meteorol. Soc., 83, 1631–1644, <https://doi.org/https://doi.org/10.1175/BAMS-83-11-1631>, 2002.

Lacroix, F., Ilyina, T., and Hartmann, J.: Oceanic CO<sub>2</sub> outgassing and biological production hotspots induced by pre-industrial river loads of nutrients and carbon in a global modeling approach, 17, 55–88, <https://doi.org/10.5194/bg-17-55-2020>, 2020.

605 Lacroix, F., Ilyina, T., Mathis, M., Laruelle, G. G., and Regnier, P.: Historical increases in land-derived nutrient inputs may alleviate effects of a changing physical climate on the oceanic carbon cycle, Glob. Chang. Biol., 27, 5491–5513, <https://doi.org/https://doi.org/10.1111/gcb.15822>, 2021a.

610 Lacroix, F., Ilyina, T., Laruelle, G. G., and Regnier, P.: Reconstructing the Preindustrial Coastal Carbon Cycle Through a Global Ocean Circulation Model: Was the Global Continental Shelf Already Both Autotrophic and a CO<sub>2</sub> Sink?, Global Biogeochem. Cycles, 35, e2020GB006603, <https://doi.org/https://doi.org/10.1029/2020GB006603>, 2021b.

Lan, X., Tans, P., and Thoning, K. W.: Trends in globally-averaged CO<sub>2</sub> determined from NOAA Global Monitoring Laboratory measurements. Version 2024-05, Noaa Gml, <https://doi.org/https://doi.org/10.15138/9N0H-ZH07>, 2024.

615 Landschützer, P., Gruber, N., Haumann, F. A., Rödenbeck, C., Bakker, D. C. E., van Heuven, S., Hoppema, M., Metzl, N., Sweeney, C., Takahashi, T., Tilbrook, B., and Wanninkhof, R.: The reinvigoration of the Southern Ocean carbon sink, *Science*, 349, 1221–1224, <https://doi.org/10.1126/science.aab2620>, 2015.

620 Landschützer, P., Gruber, N., and Bakker, D. C. E.: Decadal variations and trends of the global ocean carbon sink, *Global Biogeochem. Cycles*, 30, 1396–1417, <https://doi.org/https://doi.org/10.1002/2015GB005359>, 2016.

625 Laufkötter, C., Vogt, M., Gruber, N., Aita-Noguchi, M., Aumont, O., Bopp, L., Buitenhuis, E., Doney, S. C., Dunne, J., Hashioka, T., Hauck, J., Hirata, T., John, J., Le Quéré, C., Lima, I. D., Nakano, H., Seferian, R., Totterdell, I., Vichi, M., and Völker, C.: Drivers and uncertainties of future global marine primary production in marine ecosystem models, 12, 6955–6984, <https://doi.org/10.5194/bg-12-6955-2015>, 2015.

630 Law, R. M., Ziehn, T., Matear, R. J., Lenton, A., Chamberlain, M. A., Stevens, L. E., Wang, Y.-P., Srbinovsky, J., Bi, D., Yan, H., and Vohralík, P. F.: The carbon cycle in the Australian Community Climate and Earth System Simulator (ACCESS-ESM1) - Part 1: Model description and pre-industrial simulation, *Geosci. Model Dev.*, 10, 2567–2590, <https://doi.org/10.5194/gmd-10-2567-2017>, 2017.

Li, H. and Ilyina, T.: Current and Future Decadal Trends in the Oceanic Carbon Uptake Are Dominated by Internal Variability, *Geophys. Res. Lett.*, 45, 916–925, <https://doi.org/https://doi.org/10.1002/2017GL075370>, 2018.

635 Liao, E., Resplandy, L., Liu, J., and Bowman, K. W.: Amplification of the Ocean Carbon Sink During El Niños: Role of Poleward Ekman Transport and Influence on Atmospheric CO<sub>2</sub>, *Global Biogeochem. Cycles*, 34, e2020GB006574, <https://doi.org/https://doi.org/10.1029/2020GB006574>, 2020.

640 Lovato, T., Peano, D., Butenschön, M., Materia, S., Iovino, D., Scoccimarro, E., Fogli, P. G., Cherchi, A., Bellucci, A., Gualdi, S., Masina, S., and Navarra, A.: CMIP6 Simulations With the CMCC Earth System Model (CMCC-ESM2), *J. Adv. Model. Earth Syst.*, 14, e2021MS002814, <https://doi.org/https://doi.org/10.1029/2021MS002814>, 2022.

Maier-Reimer, E. and Hasselmann, K.: Transport and storage of CO<sub>2</sub> in the ocean - an inorganic ocean-circulation carbon cycle model, *Clim. Dyn.*, 2, 63–90, <https://doi.org/10.1007/BF01054491>, 1987.

Mauritsen, T., Bader, J., Becker, T., Behrens, J., Bittner, M., Brokopf, R., Brovkin, V., Claussen, M., Crueger, T., Esch, M., Fast, I., Fiedler, S., Fläschner, D., Gayler, V., Giorgetta, M., Goll, D. S., Haak, H., Hagemann, S., Hedemann, C., Hohenegger, C., Ilyina, T., Jahns, T., Jiménez-de-la-Cuesta, D., Jungclaus, J., Kleinen, T., Kloster, S., Kracher, D., Kinne, S., Kleberg, D., Lasslop, G., Kornblueh, L., Marotzke, J., Matei, D., Meraner, K., Mikolajewicz, U., Modali, K., Möbis, B., Müller, W. A.,  
 650 Nabel, J. E. M. S., Nam, C. C. W., Notz, D., Nyawira, S.-S., Paulsen, H., Peters, K., Pincus, R., Pohlmann, H., Pongratz, J., Popp, M., Raddatz, T. J., Rast, S., Redler, R., Reick, C. H., Rohrschneider, T., Schemann, V., Schmidt, H., Schnur, R., Schulzweida, U., Six, K. D., Stein, L., Stemmler, I., Stevens, B., von Storch, J.-S., Tian, F., Voigt, A., Vrese, P., Wieners, K.-H., Wilkenskjeld, S., Winkler, A., and Roeckner, E.: Developments in the MPI-M Earth System Model version 1.2 (MPI-ESM1.2) and Its Response to Increasing CO<sub>2</sub>, *J. Adv. Model. Earth Syst.*, 11, 998–1038,  
 655 <https://doi.org/https://doi.org/10.1029/2018MS001400>, 2019.

McKinley, G. A., Fay, A. R., Lovenduski, N. S., and Pilcher, D. J.: Natural Variability and Anthropogenic Trends in the Ocean Carbon Sink, *Ann. Rev. Mar. Sci.*, 9, 125–150, <https://doi.org/10.1146/annurev-marine-010816-060529>, 2017.

660 McKinley, G. A., Fay, A. R., Eddebar, Y. A., Gloege, L., and Lovenduski, N. S.: External Forcing Explains Recent Decadal Variability of the Ocean Carbon Sink, AGU Adv., 1, e2019AV000149,  
<https://doi.org/https://doi.org/10.1029/2019AV000149>, 2020.

Meinshausen, M., Nicholls, Z. R. J., Lewis, J., Gidden, M. J., Vogel, E., Freund, M., Beyerle, U., Gessner, C., Nauels, A.,  
 665 Bauer, N., Canadell, J. G., Daniel, J. S., John, A., Krummel, P. B., Luderer, G., Meinshausen, N., Montzka, S. A., Rayner, P. J., Reimann, S., Smith, S. J., van den Berg, M., Velders, G. J. M., Vollmer, M. K., and Wang, R. H. J.: The shared socio-economic pathway (SSP) greenhouse gas concentrations and their extensions to 2500, *Geosci. Model Dev.*, 13, 3571–3605,  
<https://doi.org/10.5194/gmd-13-3571-2020>, 2020.

670 Müller, J. D., Gruber, N., Carter, B., Feely, R., Ishii, M., Lange, N., Lauvset, S. K., Murata, A., Olsen, A., Pérez, F. F., Sabine, C., Tanhua, T., Wanninkhof, R., and Zhu, D.: Decadal Trends in the Oceanic Storage of Anthropogenic Carbon From 1994 to 2014, AGU Adv., 4, e2023AV000875, <https://doi.org/https://doi.org/10.1029/2023AV000875>, 2023.

Nakano, H., Tsujino, H., Hirabara, M., Yasuda, T., Motoi, T., Ishii, M., and Yamanaka, G.: Uptake mechanism of  
 675 anthropogenic CO<sub>2</sub> in the Kuroshio Extension region in an ocean general circulation model, *J. Oceanogr.*, 67, 765–783,  
<https://doi.org/10.1007/s10872-011-0075-7>, 2011.

Perez, F. F., Gehlen, M., Tjiputra, J. F., Olsen, A., Becker, M., Goris, N., Lopez-Mozos, M., Müller, J. D., Huertas, I. E., Chau,

T. T. T., Velo, A., Benard, G., Cainzos, V., Gruber, N., and Wanninkhof, R.: An assessment of CO<sub>2</sub> storage and sea-air fluxes  
680 for the Atlantic Ocean and Mediterranean Sea between 1985 and 2018., *Global Biogeochem. Cycles*, 2023.

Riahi, K., van Vuuren, D. P., Kriegler, E., Edmonds, J., O'Neill, B. C., Fujimori, S., Bauer, N., Calvin, K., Dellink, R., Fricko,  
O., Lutz, W., Popp, A., Cuarterma, J. C., KC, S., Leimbach, M., Jiang, L., Kram, T., Rao, S., Emmerling, J., Ebi, K., Hasegawa,  
T., Havlik, P., Humpenöder, F., Da Silva, L. A., Smith, S., Stehfest, E., Bosetti, V., Eom, J., Gernaat, D., Masui, T., Rogelj,  
685 J., Strefler, J., Drouet, L., Krey, V., Luderer, G., Harmsen, M., Takahashi, K., Baumstark, L., Doelman, J. C., Kainuma, M.,  
Klimont, Z., Marangoni, G., Lotze-Campen, H., Obersteiner, M., Tabeau, A., and Tavoni, M.: The Shared Socioeconomic  
Pathways and their energy, land use, and greenhouse gas emissions implications: An overview, *Glob. Environ. Chang.*, 42,  
153–168, <https://doi.org/https://doi.org/10.1016/j.gloenvcha.2016.05.009>, 2017.

690 Rödenbeck, C., Bakker, D. C. E., Metzl, N., Olsen, A., Sabine, C., Cassar, N., Reum, F., Keeling, R. F., and Heimann, M.:  
Interannual sea-air CO<sub>2</sub> flux variability from an observation-driven ocean mixed-layer scheme, 11, 4599–4613,  
<https://doi.org/10.5194/bg-11-4599-2014>, 2014.

695 Rödenbeck, C., DeVries, T., Hauck, J., Le Quéré, C., and Keeling, R. F.: Data-based estimates of interannual sea-air CO<sub>2</sub> flux  
variations 1957--2020 and their relation to environmental drivers, 19, 2627–2652, <https://doi.org/10.5194/bg-19-2627-2022>,  
2022.

700 Rodgers, K. B., Lee, S.-S., Rosenbloom, N., Timmermann, A., Danabasoglu, G., Deser, C., Edwards, J., Kim, J.-E., Simpson,  
I. R., Stein, K., Stuecker, M. F., Yamaguchi, R., Bódai, T., Chung, E.-S., Huang, L., Kim, W. M., Lamarque, J.-F.,  
Lombardozzi, D. L., Wieder, W. R., and Yeager, S. G.: Ubiquity of human-induced changes in climate variability, *Earth Syst.  
Dyn.*, 12, 1393–1411, <https://doi.org/10.5194/esd-12-1393-2021>, 2021.

705 Rodgers, K. B., Schwinger, J., Fassbender, A. J., Landschützer, P., Yamaguchi, R., Frenzel, H., Stein, K., Müller, J. D., Goris,  
N., Bushinsky, S. M., Chau, T. T. T., Gehlen, M., Gallego, M. A., Gloege, L., Gregor, L., Gruber, N., Hauck, J., Iida, Y., Ishii,  
M., Keppler, L., Kim, J.-E., Schlunegger, S., Sharma, S., Tjiputra, J., Toyama, K., and Vaitinada Ayar, P.: Seasonal variability  
of the surface ocean carbon cycle: a synthesis, *Global Biogeochem. Cycles*, 2023.

Sarmiento, J. L., Orr, J. C., and Siegenthaler, U.: A perturbation simulation of CO<sub>2</sub> uptake in an ocean general circulation  
model, *J. Geophys. Res. Ocean.*, 97, 3621–3645, <https://doi.org/https://doi.org/10.1029/91JC02849>, 1992.

710 Schwinger, J., Goris, N., Tjiputra, J. F., Kriest, I., Bentsen, M., Bethke, I., Ilicak, M., Assmann, K. M., and Heinze, C.:  
Evaluation of NorESM-OC (versions~1 and 1.2), the ocean carbon-cycle stand-alone configuration of the Norwegian Earth

- 715 Séférian, R., Gehlen, M., Bopp, L., Resplandy, L., Orr, J. C., Marti, O., Dunne, J. P., Christian, J. R., Doney, S. C., Ilyina, T., Lindsay, K., Halloran, P. R., Heinze, C., Segschneider, J., Tjiputra, J., Aumont, O., and Romanou, A.: Inconsistent strategies to spin up models in CMIP5: implications for ocean biogeochemical model performance assessment, Geosci. Model Dev., 9, 1827–1851, <https://doi.org/10.5194/gmd-9-1827-2016>, 2016.
- 720 Séférian, R., Nabat, P., Michou, M., Saint-Martin, D., Volodire, A., Colin, J., Decharme, B., Delire, C., Berthet, S., Chevallier, M., Sénési, S., Franchisteguy, L., Vial, J., Mallet, M., Joetzjer, E., Geoffroy, O., Guérémy, J.-F., Moine, M.-P., Msadek, R., Ribes, A., Rocher, M., Roehrig, R., Salas-y-Mélia, D., Sanchez, E., Terray, L., Valcke, S., Waldman, R., Aumont, O., Bopp, L., Deshayes, J., Éthé, C., and Madec, G.: Evaluation of CNRM Earth System Model, CNRM-ESM2-1: Role of Earth System Processes in Present-Day and Future Climate, J. Adv. Model. Earth Syst., 11, 4182–4227,  
725 <https://doi.org/https://doi.org/10.1029/2019MS001791>, 2019.
- Séférian, R., Berthet, S., Yool, A., Palmiéri, J., Bopp, L., Tagliabue, A., Kwiatkowski, L., Aumont, O., Christian, J., Dunne, J., Gehlen, M., Ilyina, T., John, J. G., Li, H., Long, M. C., Luo, J. Y., Nakano, H., Romanou, A., Schwinger, J., Stock, C., Santana-Falcón, Y., Takano, Y., Tjiputra, J., Tsujino, H., Watanabe, M., Wu, T., Wu, F., and Yamamoto, A.: Tracking  
730 Improvement in Simulated Marine Biogeochemistry Between CMIP5 and CMIP6, Curr. Clim. Chang. Reports, 6, 95–119,  
<https://doi.org/10.1007/s40641-020-00160-0>, 2020.
- Seland, Ø., Bentsen, M., Olivié, D., Tonietto, T., Gjermundsen, A., Graff, L. S., Debernard, J. B., Gupta, A. K., He, Y.-C., Kirkevåg, A., Schwinger, J., Tjiputra, J., Aas, K. S., Bethke, I., Fan, Y., Griesfeller, J., Grini, A., Guo, C., Ilicak, M., Karset, I. H. H., Landgren, O., Liakka, J., Moseid, K. O., Nummelin, A., Spensberger, C., Tang, H., Zhang, Z., Heinze, C., Iversen, T., and Schulz, M.: Overview of the Norwegian Earth System Model (NorESM2) and key climate response of CMIP6 DECK, historical, and scenario simulations, Geosci. Model Dev., 13, 6165–6200, <https://doi.org/10.5194/gmd-13-6165-2020>, 2020.
- 740 Sellar, A. A., Walton, J., Jones, C. G., Wood, R., Abraham, N. L., Andrejczuk, M., Andrews, M. B., Andrews, T., Archibald, A. T., de Mora, L., Dyson, H., Elkington, M., Ellis, R., Florek, P., Good, P., Gohar, L., Haddad, S., Hardiman, S. C., Hogan, E., Iwi, A., Jones, C. D., Johnson, B., Kelley, D. I., Kettleborough, J., Knight, J. R., Köhler, M. O., Kuhlbrodt, T., Liddicoat, S., Linova-Pavlova, I., Mizielski, M. S., Morgenstern, O., Mulcahy, J., Neininger, E., O'Connor, F. M., Petrie, R., Ridley, J., Rioual, J.-C., Roberts, M., Robertson, E., Rumbold, S., Seddon, J., Shepherd, H., Shim, S., Stephens, A., Teixiera, J. C., Tang, Y., Williams, J., Wiltshire, A., and Griffiths, P. T.: Implementation of U.K. Earth System Models for CMIP6, J. Adv. Model. Earth Syst., 12, e2019MS001946, <https://doi.org/https://doi.org/10.1029/2019MS001946>, 2020.

Silvy, Y., Frölicher, T. L., Terhaar, J., Joos, F., Burger, F. A., Lacroix, F., Allen, M., Bernadello, R., Bopp, L., Brovkin, V., Buzan, J. R., Cadule, P., Dix, M., Dunne, J., Friedlingstein, P., Georgievski, G., Hajima, T., Jenkins, S., Kawamiya, M., Kiang, N. Y., Lapin, V., Lee, D., Lerner, P., Mengis, N., Monteiro, E. A., Paynter, D., Peters, G. P., Romanou, A., Schwinger, J.,  
750 Sparrow, S., Stofferahn, E., Tjiputra, J., Tourigny, E., and Ziehn, T.: AERA-MIP: Emission pathways, remaining budgets and carbon cycle dynamics compatible with 1.5°C and 2°C global warming stabilization, 2024, 1–47, <https://doi.org/10.5194/egusphere-2024-488>, 2024.

Stock, C. A., Dunne, J. P., Fan, S., Ginoux, P., John, J., Krasting, J. P., Laufkötter, C., Paulot, F., and Zadeh, N.: Ocean Biogeochemistry in GFDL's Earth System Model 4.1 and Its Response to Increasing Atmospheric CO<sub>2</sub>, *J. Adv. Model. Earth Syst.*, 12, [https://doi.org/https://doi.org/10.1029/2019MS002043](https://doi.org/10.1029/2019MS002043), 2020.  
755

Swart, N. C., Cole, J. N. S., Kharin, V. V., Lazare, M., Scinocca, J. F., Gillett, N. P., Anstey, J., Arora, V., Christian, J. R., Hanna, S., Jiao, Y., Lee, W. G., Majaess, F., Saenko, O. A., Seiler, C., Seinen, C., Shao, A., Sigmond, M., Solheim, L., von  
760 Salzen, K., Yang, D., and Winter, B.: The Canadian Earth System Model version 5 (CanESM5.0.3), *Geosci. Model Dev.*, 12, 4823–4873, <https://doi.org/10.5194/gmd-12-4823-2019>, 2019.

Takano, Y., Ilyina, T., Tjiputra, J., Eddebar, Y. A., Berthet, S., Bopp, L., Buitenhuis, E., Butenschön, M., Christian, J. R., Dunne, J. P., Gröger, M., Hayashida, H., Hieronymus, J., Koenigk, T., Krasting, J. P., Long, M. C., Lovato, T., Nakano, H.,  
765 Palmieri, J., Schwinger, J., Séférian, R., Suntharalingam, P., Tatebe, H., Tsujino, H., Urakawa, S., Watanabe, M., and Yool, A.: Simulations of ocean deoxygenation in the historical era: insights from forced and coupled models, *Front. Mar. Sci.*, 10, 2023.

Terhaar, J.: Drivers of decadal trends in the ocean carbon sink in the past, present, and future in Earth system models, 21, 3903–3926, <https://doi.org/10.5194/bg-21-3903-2024>, 2024.  
770

Terhaar, J., Kwiatkowski, L., and Bopp, L.: Emergent constraint on Arctic Ocean acidification in the twenty-first century, *Nature*, 582, 379–383, <https://doi.org/10.1038/s41586-020-2360-3>, 2020.

775 Terhaar, J., Torres, O., Bourgeois, T., and Kwiatkowski, L.: Arctic Ocean acidification over the 21st century co-driven by anthropogenic carbon increases and freshening in the CMIP6 model ensemble, 18, 2221–2240, <https://doi.org/10.5194/bg-18-2221-2021>, 2021a.

Terhaar, J., Lauerwald, R., Regnier, P., Gruber, N., and Bopp, L.: Around one third of current Arctic Ocean primary production  
780 sustained by rivers and coastal erosion, *Nat. Commun.*, 12, 169, <https://doi.org/10.1038/s41467-020-20470-z>, 2021b.

Terhaar, J., Frölicher, T., and Joos, F.: Southern Ocean anthropogenic carbon sink constrained by sea surface salinity, *Sci. Adv.*, 7, 5964–5992, <https://doi.org/10.1126/sciadv.abd5964>, 2021c.

785 Terhaar, J., Frölicher, T. L., and Joos, F.: Observation-constrained estimates of the global ocean carbon sink from Earth System Models, 19, 4431–4457, <https://doi.org/10.5194/bg-19-4431-2022>, 2022.

Terhaar, J., Goris, N., Müller, J. D., DeVries, T., Gruber, N., Hauck, J., Perez, F. F., and Séférian, R.: Assessment of Global Ocean Biogeochemistry Models for Ocean Carbon Sink Estimates in RECCAP2 and Recommendations for Future Studies, *J.*

790 *Adv. Model. Earth Syst.*, 16, e2023MS003840, [https://doi.org/https://doi.org/10.1029/2023MS003840](https://doi.org/10.1029/2023MS003840), 2024.

Tjiputra, J. F., Schwinger, J., Bentsen, M., Morée, A. L., Gao, S., Bethke, I., Heinze, C., Goris, N., Gupta, A., He, Y.-C., Olivié, D., Seland, Ø., and Schulz, M.: Ocean biogeochemistry in the Norwegian Earth System Model version 2 (NorESM2), *Geosci. Model Dev.*, 13, 2393–2431, <https://doi.org/10.5194/gmd-13-2393-2020>, 2020.

795

Tsujino, H., Urakawa, S., Nakano, H., Small, R. J., Kim, W. M., Yeager, S. G., Danabasoglu, G., Suzuki, T., Bamber, J. L., Bentsen, M., Böning, C. W., Bozec, A., Chassignet, E. P., Curchitser, E., Boeira Dias, F., Durack, P. J., Griffies, S. M., Harada, Y., Ilicak, M., Josey, S. A., Kobayashi, C., Kobayashi, S., Komuro, Y., Large, W. G., Le Sommer, J., Marsland, S. J., Masina, S., Scheinert, M., Tomita, H., Valdivieso, M., and Yamazaki, D.: JRA-55 based surface dataset for driving ocean–sea-ice models (JRA55-do), *Ocean Model.*, 130, 79–139, <https://doi.org/https://doi.org/10.1016/j.ocemod.2018.07.002>, 2018.

Urakawa, L. S., Tsujino, H., Nakano, H., Sakamoto, K., Yamanaka, G., and Toyoda, T.: The sensitivity of a depth-coordinate model to diapycnal mixing induced by practical implementations of the isopycnal tracer diffusion scheme, *Ocean Model.*, 154, 101693, <https://doi.org/https://doi.org/10.1016/j.ocemod.2020.101693>, 2020.

805

Vaittinada Ayar, P., Bopp, L., Christian, J. R., Ilyina, T., Krasting, J. P., Séférian, R., Tsujino, H., Watanabe, M., Yool, A., and Tjiputra, J.: Contrasting projections of the ENSO-driven CO<sub>2</sub> flux variability in the equatorial Pacific under high-warming scenario, *Earth Syst. Dyn.*, 13, 1097–1118, <https://doi.org/10.5194/esd-13-1097-2022>, 2022.

810 Watson, A. J., Schuster, U., Shutler, J. D., Holding, T., Ashton, I. G. C., Landschützer, P., Woolf, D. K., and Goddijn-Murphy, L.: Revised estimates of ocean-atmosphere CO<sub>2</sub> flux are consistent with ocean carbon inventory, *Nat. Commun.*, 11, 4422, <https://doi.org/10.1038/s41467-020-18203-3>, 2020.

Wright, R. M., Le Quéré, C., Buitenhuis, E., Pitois, S., and Gibbons, M. J.: Role of jellyfish in the plankton ecosystem revealed

815 using a global ocean biogeochemical model, 18, 1291–1320, <https://doi.org/10.5194/bg-18-1291-2021>, 2021.

Yasunaka, S., Manizza, M., Terhaar, J., Olsen, A., Yamaguchi, R., Landschützer, P., Watanabe, E., Carroll, D., Adiwara, H., Müller, J. D., and Hauck, J.: An assessment of CO<sub>2</sub> uptake in the Arctic Ocean from 1985 to 2018, *Global Biogeochem. Cycles*, 2023.

820

Yukimoto, S., Kawai, H., Koshiro, T., Oshima, N., Yoshida, K., Urakawa, S., Tsujino, H., Deushi, M., Tanaka, T., Hosaka, M., Yabu, S., Yoshimura, H., Shindo, E., Mizuta, R., Obata, A., Adachi, Y., and Ishii, M.: The Meteorological Research Institute Earth System Model Version 2.0, MRI-ESM2.0: Description and Basic Evaluation of the Physical Component, *J. Meteorol. Soc. Japan. Ser. II*, 97, 931–965, <https://doi.org/10.2151/jmsj.2019-051>, 2019.

825

Zeng, J., Iida, Y., Matsunaga, T., and Shirai, T.: Surface ocean CO<sub>2</sub> concentration and air-sea flux estimate by machine learning with modelled variable trends, *Front. Mar. Sci.*, 9, 2022.

830 Ziehn, T., Chamberlain, M. A., Law, R. M., Lenton, A., Bodman, R. W., Dix, M., Stevens, L., Wang, Y.-P., and Srbinovsky, J.: The Australian Earth System Model: ACCESS-ESM1.5, *J. South. Hemisph. Earth Syst. Sci.*, 70, 193–214, 2020.